

1 **Chemical and U-Sr isotopic variations in stream and source waters of the Strengbach**
2 **watershed (Vosges mountains; France)**

3 ¹Pierret M.C., ¹Stille P., ¹⁻²Prunier J., ¹Viville D. and ¹Chabaux F.

4

5 (1) Laboratoire d'Hydrologie et de Géochimie de Strasbourg, EOST, Université de
6 Strasbourg/CNRS, 1 rue Blessig 67084 Strasbourg, France.

7 (2) Present address LMTG – Université Paul Sabatier, CNRS/IRD, Observatoire Midi-
8 Pyrénées, 14, avenue Edouard Belin, 31400 Toulouse, France.

9

10 Correspondence to: Marie Claire Pierret marie-claire.pierret@unistra.fr

11

12 **Abstract**

13 This is the first comprehensive study dealing with major and trace element data as well as ⁸⁷Sr/⁸⁶Sr
14 isotope and (²³⁴U/²³⁸U) activity ratios (AR) determined on the totality of springs and brooks of the
15 Strengbach catchment. It shows that the small and more or less monolithic catchment drains
16 different sources and streamlets with very different isotopic and geochemical signatures. Different
17 parameters control the diversity of the source characteristics. Of importance is especially the
18 hydrothermal overprint of the granitic bedrock, which was stronger for the granite from the northern
19 slope; also significant are the different meteoric alteration processes of the bedrock causing the
20 formation of 0.5 to 9 meter thick saprolite and above the formation of an up to 1m thick soil system.
21 These processes mainly account for springs and brooks from the northern slope having higher
22 Ca/Na, Mg/Na, Sr/Na ratios but lower ⁸⁷Sr/⁸⁶Sr isotopic ratios than those from the southern slope.
23 The chemical compositions of the source waters in the Strengbach catchment are only to a small
24 extent the result of alteration of primary bedrock minerals and rather reflect
25 dissolution/precipitation processes of secondary mineral phases like clay minerals.

26 The ($^{234}\text{U}/^{238}\text{U}$) AR, however, are decoupled from the $^{87}\text{Sr}/^{86}\text{Sr}$ isotope system and reflect to some
27 extent the level of altitude of the source and, thus, the degree of alteration of the bedrock. The
28 sources emerging at high altitudes have circulated through already weathered materials (saprolite
29 and fractured bedrock depleted in ^{234}U) implying ($^{234}\text{U}/^{238}\text{U}$) AR <1 , which is uncommon for surface
30 waters. Preferential flow paths along constant fractures in the bedrocks might explain the over time
31 homogeneous U AR of the different spring waters. However, the geochemical and isotopic
32 variations of stream waters at the outlet of the catchment are controlled by variable contributions of
33 different springs depending on the hydrological conditions.

34 It appears that the ($^{234}\text{U}/^{238}\text{U}$) AR is an appropriate very important tracer for studying and
35 deciphering the contribution of the different source fluxes at the catchment scale because this
36 unique geochemical parameter is different for each individual spring and at the same time remains
37 unchanged for each of the springs with changing discharge and fluctuating hydrological conditions.
38 This study further highlights the important impact of different and independent water pathways in
39 fractured granite controlling the different geochemical and isotopic signatures of the waters. Despite
40 the fact that soils and vegetation cover have a great influence on the water cycle balance
41 (evapotranspiration, drainage, runoff), the chemical compositions of waters are strongly modified
42 by processes occurring in deep saprolite and bedrock rather than in soils along the specific water
43 pathways.

44

45 Keywords: U activity ratios, Sr isotopes, spring and stream water chemistry, weathering,
46 Strengbach catchment.

47

48 **1. Introduction**

49 Large rivers carry erosion products from the different drainage areas and, therefore, are pathways of
50 continental weathering products that finally enter the oceans. Thus, they fetch the various chemical
51 and isotopical characteristics of the different drainage basins and, therefore, allow to elucidate

52 erosion processes, derive erosion rates and to illustrate biogeochemical cycling of elements. Many
53 of the major world rivers are well documented with major and trace element and isotope data on
54 dissolved and suspended phases, which provide the different factors controlling chemical and
55 physical denudation (Degens et al., 1991; Dupré et al., 2003; Gaillardet et al., 1999; Martin and
56 Meybeck, 1979 ; Négrel et al., 1993). At the large catchment scale, the stream waters chemical
57 composition is generally the result of mixing between phases derived from the different main
58 lithologies (e.g., Bickle et al., 2006; Blum et al., 1998; Chabaux et al., 2001; Millot et al., 2003;
59 Steinmann and Stille, 2009; Tipper et al., 2006; Zakharova et al., 2007). The impact and the role of
60 vegetation cover and soils on the chemical or isotopical evolution of erosion signals in waters of
61 small catchments have very recently ~~only seldom~~ been discussed (Laudon et al., 2004; Cenko-Tok et
62 al., 2009; Cidivini et al., 2011; Engstrom et al., 2010; Kohler et al., 2014; Lemarchand et al., 2010;
63 Zakharova et al., 2007). Determination of parameters controlling the chemical composition of
64 superficial waters is important for a correct modeling of the future evolution of ecosystems in
65 response to external natural or anthropogenic forcing such as climate evolution and atmospheric
66 pollution (trace metal depositions, acid rain etc.). Among these parameters water/rock interactions
67 (including secondary phases such as clays), hydrological processes and biological activities play an
68 important role in affecting mobilization, (re)cycling and fractionation of elements; their specific
69 influences on weathering processes at the watershed scale remains a matter of discussion (Brantley
70 et al., 2008).

71 Because natural systems are subject to complex and multiple reactions, the combination of different
72 geochemical and isotopical tools is necessary to decipher the different natural processes. $^{87}\text{Sr}/^{86}\text{Sr}$
73 isotopic ratios and ($^{234}\text{U}/^{238}\text{U}$) AR have successfully been used in the discussion of hydrological and
74 hydrochemical processes at the catchment scale (e.g. Riotte and Chabaux, 1999; Tricca et al., 1999;
75 Aubert et al., 2002; Bagard et al., 2011; Bickle et al., 2005; Bonotto and Andrews, 2000; Chabaux
76 et al., 2011; Durand et al., 2005; Schaffhauser et al., 2014). Indeed, when the U system has been
77 closed for approximately 1 million years, minerals and rocks are in secular equilibrium and

78 activities of all parents and daughters from ^{238}U decay chain are identical and the ($^{234}\text{U}/^{238}\text{U}$) AR is
79 equal to 1. However, this ratio can fractionate during chemical weathering when ^{234}U is more easily
80 released into solution by the combined effects of 1) direct recoil of ^{234}Th near grain boundaries out
81 of mineral and 2) preferential release from crystal lattices that are damaged by energetic α -decay
82 (e.g. Bourdon et al., 2009; Chabaux et al., 2003; 2008; DePaolo et al., 2006; 2012; Osmond and
83 Ivanovich, 1992 and references therein). Therefore, natural waters (stream, spring, groundwaters,
84 seawaters) are generally in excess of ^{234}U with ($^{234}\text{U}/^{238}\text{U}$) AR >1 (Andrews and Kay, 1983;
85 Camacho et al., 2010; Chabaux et al., 2003, 2008; Dosseto et al., 2008, 2012; Gryzmko et al., 2007;
86 Osmond and Ivanovich, 1992; Paces et al., 2002; Pierret et al., 2012; Vigier et al., 2001, 2006).
87 Consequently, ($^{234}\text{U}/^{238}\text{U}$) AR in superficial waters allow to identify river- flow patterns, and
88 hydrological mixing by tracing the sources of water and recording mixing between superficial and
89 groundwaters characterized by different U AR. Thus the ($^{234}\text{U}/^{238}\text{U}$) AR change along river flows
90 and in function of hydrological mixing (e.g., Chabaux et al., 2001; Durand et al., 2005; Maher et al.,
91 2006; Osmond and 1982; Paces et al., 2002; Riotte et Chabaux, 1999).

92 In the present paper we focus on a small, more or less monolithic drainage basin, the experimental
93 Strengbach catchment (Vosges mountains, NE France). Several studies have shown that the
94 vegetation cover, the atmospheric deposition, the secondary minerals and the biological recycling
95 play an important role in controlling the geochemical signatures of soil solutions (Brioshi et al.,
96 2012; Lemarchand et al., 2010; Lemarchand et al., 2012; Prunier, 2008; Stille et al., 2006, 2009,
97 2011, 2012). The impact of physico-chemical processes in soil on the chemical balance of waters at
98 the outlet is rather weak. For instance, the mean annual flux of Ca in soil solution at 60 cm depth
99 represents 5 to 20% of the annual flux at the outlet, depending on the type of vegetation or soil
100 (Cenki-Tok et al., 2009). Therefore, the chemical compositions of waters are mainly controlled by
101 interactions occurring with the deep saprolite and bedrock rather than with soils.

102 A previous U isotope study performed on waters from the Strengbach streamlet shows a decrease of
103 the ($^{234}\text{U}/^{238}\text{U}$) AR from 1.02 to 0.96 when the discharge of the stream increases (Riotte and

104 Chabaux, 1999). Such an isotopic evolution has been interpreted as mixing between a water body
105 enriched in ^{234}U , which is supposed to have interacted with a granitic bed rock at secular
106 equilibrium, and waters with a ($^{234}\text{U}/^{238}\text{U}$) AR below unity pointing to mobilization of U from
107 material that has already been weathered. Similarly, the streamlets $^{87}\text{Sr}/^{86}\text{Sr}$ isotope ratios collected
108 during low flow periods have low $^{87}\text{Sr}/^{86}\text{Sr}$ ratios than during high water flow events (Aubert et al.,
109 2002). The Sr signature at low discharge has been explained by important contributions of waters
110 from the deep soil profile during the recession stage, whereas higher $^{87}\text{Sr}/^{86}\text{Sr}$ isotope ratios at
111 higher discharge are due to important contributions of waters from the saturated area of the
112 catchment.

113 In order to define more precisely temporal and spatial variations of the hydrochemistry of the
114 streamlet and the different springs and to evaluate the major and trace element sources and the
115 processes controlling this element supply to the freshwaters, additional ($^{234}\text{U}/^{238}\text{U}$) AR, $^{87}\text{Sr}/^{86}\text{Sr}$
116 isotopic ratios and major and trace element concentrations were analyzed in the different source
117 waters collected during two different hydrological seasons (2004-2006) and compared to those of
118 the streamlet.

119

120 **2. Site description**

121 The Strengbach catchment is a small granitic watershed (0.8 km²) where meteorological,
122 hydrological and geochemical data are recorded since 1986 (Observatoire Hydro-Géochimique de
123 l'Environnement; OHGE; <http://ohge.u-strasbg.fr>). The first studies were performed in order to
124 understand the impact of acid rain on the forested ecosystem (Dambrine et al. 1991, 1992a,b; Probst
125 et al. 1990, 1992a, b). The catchment is situated in the Vosges Mountains (NE France) at altitudes
126 between 880 and 1150 m (amsl) and has strongly inclined slopes (mean 15°; Fig. 1).

127 The climate is temperate oceanic mountainous (mean annual temperature of 6°C; mean monthly
128 temperature range from -2 to 14°C) with an average rainfall of 1400 mm/yr (ranging between 890
129 and 1630 mm/yr over the period 1986-2006) and with snowfall during 2-4 month/yr (Probst and

130 Viville, 1997; Viville et al., 2012; OHGE Data). The mean annual runoff for the same period is of
131 853 mm ($26.9 \text{ L s}^{-1} \text{ km}^{-2}$) and ranges from 525 to 1147 mm over 1986-2006 (Ladouche et al., 2001;
132 Probst and Vivile, 1997; OHGE data). The evapotranspiration (ETP) has been evaluated to be about
133 40% on the site (Aubert, 2001; Probst et al., 1992).

134 The bedrock is mainly composed of a Hercynian base-poor granite ($332 \pm 2 \text{ Ma}$) (Boutin et al.,
135 1995), with low Ca and Mg contents (less than 1% for both); it suffered different degrees of
136 hydrothermal alteration some 180 Ma ago (Fichter et al., 1998). In addition to the granite, which is
137 strongly hydrothermally altered on the northern slope and comparatively weakly altered on the
138 southern slope, small microgranite and gneiss bodies outcrop at the southern and northern slopes
139 (Fig.1) (El Gh'mari, 1995; Fichter et al., 1998). The gneiss is enriched in Mg mainly because of the
140 presence of biotite and chlorite (El Gh'mari, 1995; Fichter, 1997). Hydrothermal processes caused
141 the alteration and transformation of albite, K-feldspar and muscovite into fine-grained illite and
142 quartz; biotite and albite disappeared to a large extent. The strongly altered granite (on the northern
143 slope) is characterized by larger amounts of quartz, clays and Fe-oxides, small amounts of apatite
144 (<1%), and by higher Mg but lower Ca, K and Na contents than the less altered granite at the
145 southern slope (El Gh'mari, 1995; Fichter et al., 1998). In addition, the northern sun-facing slope is
146 characterized by a drier and slightly warmer climate with 10% less precipitation than observed for
147 the southern slope. The soils are brown acidic to ochreous brown podzolic and are generally about 1
148 meter thick. They are very coarse grained, sandy and rich in gravel (Fichter et al., 1998). The brown
149 acidic soils are mainly located on the northern slope and are characterized by higher clay contents,
150 lower K-feldspar, lower albite, higher cation exchange capacity (CEC), lower pH and lower organic
151 matter content than the ochreous brown podzolic soils, which are mainly located on the southern
152 slope (Fichter 1997; Fichter et al., 1998). The pedological differences are due to the different
153 mineralogical compositions of the northern and southern bedrocks, and the different types of
154 vegetation but also the different orientations of the slopes. Indeed, exposure and consequently
155 rainfall and temperature influence the chemical weathering of soils and organic matter, the soil

156 acidity and processes of clay formation (Egli et al., 2007; 2010).

157 A sandy saprolite separates soil and granite. Its thickness varies between 1 and 9 meters; on the
158 southern slope it is generally thicker (El Gh'Mari, 1995) with the most important thickness in the
159 depression zone near the four springs CS1, CS2, CS3 and CS4. The forest covers 90% of the area
160 and corresponds to about 80% spruce (mainly *Piceas Abies L.*) and 20% beech (*Fagus Sylvatica*).

161 The catchment contains 10 different springs feeding the Strengbach streamlet (Fig.1).

162 The catchment is situated in a remote area lacking direct industrial activities. Nevertheless,
163 atmospheric pollution occurs in many forms (acidic deposition, O₃ pollution or as atmospheric dust
164 deposition). Anthropogenic Pb has been identified in the atmospheric dust depositions and soils
165 (Lahd Geagea et al., 2008b; Stille et al., 2011). The forestry has increased the proportion of spruce
166 with especially dense spruce plots planted between 1890 and 1960. The site is well equipped for
167 sampling of atmospheric depositions and spring and stream waters at the whole catchment scale.

168 For this study, the stream and the different springs of the catchment were collected at various
169 hydrological periods with high and low water levels during a two years period (2004-2006) in order
170 to obtain a precise chemical and isotopic signature of the different sources in this hydrological
171 system (Fig. 1). The springs SG, ARG, RH, BH, CS₃ and CS₄ are located on the northern slope and
172 the springs CS₁, CS₂, SH and RUZS emerge at the southern slope (Fig. 1). The spring RUZS is
173 situated in the humid zone at the bottom of the catchment near the outlet (saturated area, Fig.1) and
174 covered by dense grass vegetation. In addition rain (bulk precipitation) and throughfalls were
175 collected using rain collectors and gutters, respectively.

176

177 **3. Analytical procedures**

178 The different spring waters were collected every 6 weeks during 2 years unless the springs were dry
179 or under snow. The waters were collected in clean polyethylene (HDPE) bottles (250 ml for major
180 element analysis and 1 liter for isotope and trace element analysis) and filtered the same day
181 through a 0.45 μ m pore diameter membrane (Millipore ester cellulose, 142 mm diameter). Before,

182 the HDPE bottles were washed with HCl 10% (24h contact) and then rinsed with MilliQ deionised
183 water. The filtrated waters for trace element and U-Sr isotopic composition determinations were
184 acidified with 250 μ l of ultrapure HNO₃ 13M and then stored in a cold room at 5°C.

185 The pH were measured just after filtration using a pHM210 MeterLab (Radiometer analytical) with
186 an Mettler HA405-DXKS8 electrode and calibrated with standard buffer solutions (pH 4.00 and
187 7.00 at 25°C). The precision of the pH measurement was \pm 0.02 units. The electrical conductivity
188 and the alkalinity were determined respectively using a CDM210 MeterLab (radiometer analytical)
189 with an CDC 745-9 electrode (precision 0.1 μ S/cm) and with 716DMS Titrino (Metrohm ; precision
190 of 0.01 meq/l – Acid/base titration, Gran method).

191 The major element contents were determined by ionic chromatography, atomic absorption,
192 colorimetry and ICP-AES and the trace element concentrations were determined by ICP-MS
193 (Pierret et al., 2010, Chabaux et al., 2011). The analytical uncertainty of the major cation and anion
194 determinations in solution (by atomic absorption and ionic chromatography Dionex, 4000 I) is \pm 2
195 %. The uncertainty on the major element concentrations such as Fe, Al, Mn and Si (by ICP-EAS,
196 Jobin Yvon 124) is \pm 5%, and that of the trace element concentrations (by ICP-MS, VG Plasma
197 Quad; Thermo Electron) is \pm 5%. The dissolved organic carbon (DOC) was determined using an
198 organic carbon analyser (Shimadzu TOC-5000A) with an uncertainty of 5 to 10 %, The accuracy of
199 the analysis was assessed by regular analysis of the SLRS-4 riverine standards,

200 The Sr isotopic ratios were determined by thermo-ionisation mass spectrometry on a multi-collector
201 VG-Sector mass spectrometer. Sr was extracted by standard procedures (Steinmann et Stille, 1997;
202 Lahd Geagea et al., 2008a; Pierret et al., 2010). The routinely measured NBS 987 standard yield an
203 average ⁸⁷Sr/⁸⁶Sr ratio of 0.71026 ± 0.00002 (2s) for 10 determinations during the course of this
204 study. The U isotope ratios were analysed on a TRITON Thermofinnigan mass spectrometer after
205 separation and purification of U by anionic exchange chromatography (resin AG1X8, 200-400
206 mesh) following the classical technique used in the lab (e.g. Chabaux et al., 1997; Pelt et al., 2008,
207 Pierret et al., 2012). During this study (2006-2008) the reproducibility of the U isotopic analyses

208 was tested with the HU1 standard which yield an average value of 0.999 ± 0.004 (2σ) ($n=27$). The
209 analytical error for the ($^{234}\text{U}/^{238}\text{U}$) activity ratio is $\pm 0.5\%$ (2σ).

210

211 **4. Results**

212 Previous studies performed on the Strengbach watershed mainly focused on the geochemical and
213 isotopic variations of dissolved loads of the stream waters collected at its outlet. The new results
214 (Tables 1 and 2) yield a first complete dataset of the spatial variability of major and trace element
215 concentrations as well as Sr and U isotope ratios of the spring and streamlet waters emerging on the
216 Strengbach watershed. The data also allow us to present the geochemical variability of the source as
217 well as stream waters at the outlet of the watershed over the period 2004-2006, that is to say during
218 two hydrologic cycles.

219

220 **4.1. The major and trace element data**

221 Among the spring and stream waters the pH, alkalinity, DOC, TDS_w (total dissolved solids, table
222 1), TDS-Ca (total dissolved solids-cation; table 1) and conductivity are highly variable and range
223 respectively from 5 to 6.85, from 0 to 0.16 meq/L, from 0.42 to 11.6 ppm, from 10.3 to 26.8 mg/L,
224 from 3.87 to 9.05 mg/L, and from 13.2 to 60.3 $\mu\text{S}/\text{cm}$ (Table 1). The pH is well correlated with
225 alkalinity and TDS-Ca (Fig. 2). The range of variations of the major element concentrations at the
226 watershed scale can be important but clearly depends on the chemical elements and the physico-
227 chemical parameters. For the cation concentrations the variation at the watershed scale reaches
228 about one order of magnitude for Mg, but only 20 to 30% for Na concentrations. At the watershed
229 scale, the most discriminating cation is Mg. SH and CS₁ sources are marked by weakest Mg and Ca
230 and the SG source by highest concentrations (Table 1). In addition, as illustrated by Ca/Na, Mg/Na
231 and $\text{H}_4\text{SiO}_4/\text{Ca}$ concentration ratios (Fig.3) but also the K/Na, Sr/Na, Mg/Ca ratios (not shown), the
232 different springs are not only marked by different mean major element concentrations (2004-2006
233 period) but also by different elemental ratios.

234 The data points of the different sources define linear trends with slopes different from each other
235 (Fig. 3). The variation of the Ca/Na and Mg/Na ratios are much larger at the watershed scale than at
236 the scale of a single spring. On the basis of the above data a clear distinction is possible between the
237 spring waters from the northern slope (SG, RH, ARG, CS₃, CS₄ and BH) and those from the
238 southern slope (CS₁, CS₂, SH and RUZS), the former being characterized by higher pH, alkalinity,
239 conductivity TDSw and Ca/Na, K/Na and Mg/Na ratios than the latter (Figs. 2 and 3; table 1). In
240 addition to the spatial variations, the chemical signatures of waters also show temporal variations.
241 These are strongest for the most DOC enriched sources (RUZS, SH) and for the stream at the outlet
242 (RS).

243

244 **4.2. Sr and U isotope data**

245 The ⁸⁷Sr/⁸⁶Sr isotopic composition values of the different spring waters are highly variable and
246 range between 0.72206 (RH) and 0.72801 (SH) with an average Sr isotopic composition for the
247 stream at the outlet of 0.72573 (Fig. 4, Table 1). The data show a clear relationship between the Sr
248 isotopic signature and the geographical location in the watershed; the springs from the northern
249 slope are characterized by lower ⁸⁷Sr/⁸⁶Sr ratios and higher Sr concentrations (Fig. 4).

250 As shown in Fig.6, the variation range of (²³⁴U/²³⁸U) AR in the source waters is much larger than
251 that of the streamlets waters at the outlet. The U AR range from 1.112 (BH) to 0.819 (CS3); the
252 average (²³⁴U/²³⁸U) AR for the stream at the outlet is 1.104. Among the 9 springs analyzed, 8 of
253 them have unusual low (²³⁴U/²³⁸U) AR <1. In addition, and to the best of our knowledge, these
254 values are the lowest ever published before for superficial waters. Indeed, the U AR measured in
255 world surface rivers or groundwaters have generally (²³⁴U/²³⁸U) >1 (see introduction and citations
256 therein).

257 In contrast to Sr isotopic compositions (Fig. 6) or chemical concentrations (Fig. 3) (²³⁴U/²³⁸U) AR
258 of a single source do not significantly vary over the period 2004-2006 (Fig 7). Finally, ⁸⁷Sr/⁸⁶Sr and
259 ²³⁴U/²³⁸U AR of the source waters are not correlated with each other and in contrast to the Sr

260 isotopic compositions or chemical concentrations (Fig 6) there is no clear distinction between the U
261 AR of the springs from the southern and northern slope. In the Strengbach watershed there is a clear
262 increase of the U AR of the source waters when the altitude of the spring decreases. A similar
263 behavior has been observed for waters from another small granitic watershed in the Vosges
264 Mountain, the Ringelbach watershed (Schaffhauser et al., 2014). But in contrast to the Ringelbach
265 catchment, where the U AR in the spring waters are above 1, one observed for the spring waters of
266 the Strengbach catchment $U AR \leq 1$ except for BH source.

267

268 **5. Discussion**

269

270 **5.1 Geochemical and Sr isotopic characteristics of the spring waters:**

271 As shown in the result section, the chemical characteristics of the sources are marked by an
272 important spatial variation with in particular a clear distinction between the springs from the
273 northern and the southern slope (Fig. 3), It appears that the Ca/Na, Mg/Na, and H_4SiO_4/Na
274 concentration ratios are neither rainwater nor throughfall controlled. Indeed rainwater and
275 throughfall show rather large variations of their Ca/Na or Mg/Na ratios (throughfall: Ca/Na: 0.9-
276 2.1; Mg/Na: 0.3-0.6) and do not plot at one of the extremities of the correlations. Mass balance
277 calculations show that the atmospheric input (including rain and throughfalls) corresponds to various
278 proportion of the exportation flux at the watershed scale, depending on type of element, as for
279 example 2%, 8% or 19 % for Si, U or Sr respectively (Table 3).

280 Similarly, the observation of a clear increase of the Sr isotope ratios with increasing discharge
281 towards values different from those of rainwater and/or throughfall Sr isotopic composition values
282 ($^{87}Sr/^{86}Sr$ ratios of 0.71110, 0.71327 and 0.71293 for rain, throughfall under spruces and throughfall
283 under beeches respectively) implies that rainwater or throughfall cannot be a significant source of
284 cation fluxes in the spring waters (Figs.7a and c and 13).

285 Therefore, chemical differences among the sources of the Strengbach watershed have to be
286 interpreted in terms of variations in the nature or in the intensity of water-rock interactions
287 occurring from one source to another or in the intensity of the interactions between different water
288 reservoirs. This interpretation is entirely consistent with the correlations observed for the spring
289 waters at the watershed scale between the alkalinity, TDS_w and their pH (Fig. 2; Table 1), since
290 consumption of H⁺ during silicate weathering increases pH and alkalinity. Thus, from these data it
291 appears, that the spring waters from the northern slope with higher total dissolved solid contents,
292 higher alkalinity and pH values (SG, CS4, CS3, RH with BH having the highest values) are more
293 involved in weathering reactions, or are subject to more intense weathering processes than spring
294 waters from the southern slope (especially SH, RUZS and CS1).

295 The geochemical signatures of the different springs can be generally linked to specific lithological
296 and mineralogical differences existing for the two hillsides of the catchment. This is particularly
297 obvious for the SG spring, which emerges near the top of the catchment, just below the gneiss,
298 whereas the other sources emerge within the granitic environment (Fig. 1). In comparison with the
299 granite, the gneiss has 4 to 5 times higher Mg concentrations due to important occurrences of biotite
300 and chlorite (El Gh'mari, 1995; Table 4). The Mg/Na and Mg/Ca elemental ratios are about 7.5
301 respectively 11 for the gneiss and range from 0.7 to 0.1 respectively 0.5 to 1.5 for the granite (El
302 Gh'Mari, 1995; Fichter, 1997; Table 4). Mg is also more concentrated in the gneiss-derived soils
303 (MgO : 0.9 to 1.4 wt.%), than in other soil profiles of the catchment (0.4 to 0.7 wt.%) (El Gh'Mari,
304 1995; Lefèvre, 1988; Table 4). Similarly, the Ca/Na ratios of the gneiss (0.71) and the
305 corresponding soils (0.7 to 9.2) are higher than those of the granite (0.2 to 0.6) or of the
306 corresponding soils (0.1 to 0.5) (El Gh'Mari, 1995; Fichter, 1997; Table 4). All these lithological
307 and pedological characteristics explain why the SG spring waters are more enriched in Mg and have
308 higher Mg/Ca, Mg/Na and Ca/Na ratios than the other springs (Fig. 3).

309 The variation of the chemical data of the other spring waters emerging from the granite might result
310 from the specific characteristics of the two hillsides, which show different types and thicknesses of

311 soils and saprolite and different degrees of hydrothermal alteration of the granitic bedrock (Lefèvre,
312 1988; Fichter, 1997; El Gh'Mari, 1998; see also geological setting). Indeed, the study of 13
313 weathering profiles from the whole Strengbach catchment point to important variations of the
314 mineralogical composition of soils and bedrocks at the catchment scale (El Gh'Mari, 1995; Fichter,
315 1997; Aubert 2001; Prunier, 2008; Stille et al. 2009). The soils from the northern slope are brown
316 acidic and overlay a 0.5 to 4 m thick saprolite. At the southern slope, however, an ochreous
317 podzolic soil type overlays a much thicker 4 to 9 m deep saprolite (El Gh'mari, 1995; Fichter et al.,
318 1998). The bedrock from the northern slope was subjected to stronger hydrothermal alteration,
319 which caused disappearance of albite and biotite, diminution of K-feldspar but an increase of
320 quartz, clays and white mica contents and the occurrence of hematite (Bonneau, 1994; Fichter,
321 1997; El Gh'Mari, 1995). The hydrothermally strongly altered granite on the northern slope is
322 characterized by generally higher Mg and lower Ca and Na contents than observed for the less
323 altered granite on the southern slope (Fichter et al., 1998. El Gh'Mari, 1995; Table 4). This could
324 account for the comparatively higher Mg concentrations and Mg/Na ratios of the sources from the
325 northern slope, but not for e.g. the higher Ca or K concentrations.

326 The $^{87}\text{Sr}/^{86}\text{Sr}$ ratios of springs from the southern slope (SH, CS₂, CS₁, RUZS) are, like the
327 corresponding rocks and soils (Aubert et al. 2002) (Fig. 7), more radiogenic with lower Sr
328 concentrations than those from the northern slope (BH, RH, SG, CS₃, CS₄) (Fig. 4). Thus, the Sr
329 isotopic compositions of springs can be directly related to the signatures of the weathering profile
330 and their geographical localization. But the mineral phases involved in the weathering processes
331 and causing the geochemical characteristics of these superficial waters are still matter of discussion.
332 Based on Sr and Nd isotope ratios, Aubert et al. (2001) explained the isotopic signature of the
333 Strengbach stream water by mixing of two isotopically different end-members: apatite and
334 plagioclase. However, the Mg/Sr and Mg/Ca ratios of the waters cannot simply be explained by
335 dissolution of apatite and plagioclase (Fig. 8a,b). In addition, biotite and muscovite have far too
336 high Sr isotopic ratios (respectively 5.8 and 5.4; Aubert et al., 2001) and thus their contribution can

337 be ignored. The clay fractions, extracted from the two weathering profiles at sites HP and VP
338 (Prunier, 2008) can represent an end-member able to explain the Sr isotopic composition as well as
339 the Mg/Ca and Mg/Sr ratios of springs. The springs, bulk soils and clays from the southern slope
340 show higher $^{87}\text{Sr}/^{86}\text{Sr}$ ratios than those from the northern slope. Clay fraction contents in weathering
341 profiles from northern slope are twice as big as those from the southern slope. This suggests that the
342 impact of clay on the chemical composition of springs and streams is more important on the
343 northern than the southern slope. This also explains why the springs from the northern slope are
344 more radiogenic (Fig. 4a and b) with comparatively higher Mg/Ca and Mg/Sr ratios (Fig. 8a and b)
345 than those from southern slope.

346 Such an interpretation is consistent with results of numerical modeling, which indicates that
347 precipitation/dissolution of more or less crystallized clay minerals (such as smectite) control the Mg
348 concentrations and possibly the high Mg/Ca ratios in the source waters of the Strengbach watershed
349 (Godderis et al. 2006; 2009). The same authors proposed that Mg^{2+} is controlled by smectites, Ca^{2+}
350 by the dissolution of apatite and by smectite, and K^+ by smectite/illite precipitation and dissolution
351 of K-feldspar. Interaction with clays might occur all along the circulation pathway of waters in
352 soils, saprolite and in bedrock fractures. Recent studies in the Mule Hole watershed, Mackenzie
353 basin and Damma Glacier catchment confirm the importance of secondary mineral formation,
354 especially montmorillonite in the control of chemical composition of stream water at the watershed
355 scale (Violette et al., 2010; Beaulieu et al., 2011; Hindshaw et al., 2011).

356 Thus, the variation of the current chemical compositions of the source waters in the Strengbach
357 catchment possibly reflects dissolution/precipitation processes of secondary mineral phases like
358 clay minerals. In such a model the low apatite-like Sr isotopic composition values of the source
359 waters and comparatively high and not apatite-like Mg/Ca ratios can be explained by the fact that
360 the Sr has not been remobilized by alteration of primary apatite but by weathering of secondary
361 mineral phases, which integrated during an earlier stage of alteration and crystallization apatite-

362 derived Sr. At this point we therefore propose that the alteration flux controlling the $^{87}\text{Sr}/^{86}\text{Sr}$ and
363 Mg/Ca (resp Mg/Sr) variation in the sources is imposed by secondary minerals.

364

365 **5.2. $^{234}\text{U}/^{238}\text{U}$ AR in spring waters**

366 Observation of ($^{234}\text{U}/^{238}\text{U}$) AR < 1 in most of the spring and stream waters of the Strengbach
367 catchment is unusual as river waters exhibit generally ^{234}U excess (e.g., Chabaux et al., 2003). U AR
368 < 1 have already been observed for waters from the outlet of the Strengbach catchment (0.963 to
369 1.023) with a decrease of the U AR in the dissolved load when the discharge increases (Riotte et al.,
370 1999). The authors explained this variation by the involvement of different weathered end-
371 members: a water body enriched in ^{234}U which weathered the granitic bedrock at secular
372 equilibrium and waters with a U AR below unity representing mobilization of U from material that
373 has already been weathered. Our study shows an even larger range of variation of the U AR among
374 the different springs ranging from 0.819 (CS3) to 1.112 (BH) (Table 2). The lack of correlation
375 between ($^{234}\text{U}/^{238}\text{U}$) AR and $^{87}\text{Sr}/^{86}\text{Sr}$ isotopic compositions or chemical values (Fig. 5a and b) show
376 that AR are not simply lithology controlled.

377 The mechanisms classically involved to explain ($^{234}\text{U}/^{238}\text{U}$) AR >1 in natural waters are linked to the
378 recoil process associated to the decay of ^{238}U : 1) due to alpha recoil when ^{238}U decays to ^{234}Th , it can
379 be ejected out of a grain into the fluid if the distance to the grain boundary is smaller than the recoil
380 range of ^{234}Th (~30 nm; DePaolo et al., 2006); the ^{234}Th decays then rapidly to ^{234}U (^{234}Th half-life is
381 24 days); (2) α - particles emitted during radioactive decay damage the crystal lattice of mineral
382 grains and the recoil nuclide is subsequently easily mobilized out of the damaged site. As a
383 consequence, the daughter nuclide ^{234}U is preferentially leached relative to the parent ^{238}U during
384 weathering. Thus, natural waters with ($^{234}\text{U}/^{238}\text{U}$) AR < 1 most likely correspond to environments,
385 which have already experienced a loss of ^{234}U .

386 One might simply suggest that the U AR < 1 in the Strengbach source waters are the results of
387 circulation through already weathered soils, supposedly having U AR < 1 due to previous

388 weathering. However, chemical flux balance calculations show that the annual U fluxes from the
389 soils under spruces or beech trees represent at maximum about 8% or 22%, respectively, of the
390 annual U flux at the outlet (Table 3). At the same time, the U concentrations in the different
391 springs can reach on average 0.345 ppb whereas they range only between 0.011 to 0.023 ppb
392 (factor of 30 to 15 lower) in the deep soil solutions of the two experimental plots (Table 2). In
393 addition, ($^{234}\text{U}/^{238}\text{U}$) AR determined on soil solutions from depths between 5 and 70 cm, range from
394 0.899 and 0.945 under spruces and from 0.953 to 1.194 under beech trees (Prunier, 2008) whereas
395 they are significantly low for some spring waters (0.82). This indicates that circulations and
396 interactions in the saprolite and bedrock (below the soil) control the U isotopic signature in
397 spring and stream waters.

398 The relationship between the U AR and the altitude of the springs (Fig. 9) indicates that the springs
399 from both slopes with the lower U AR (CS1, CS2, CS3, CS4) are located at higher altitude and
400 circulate in zones where the saprolite reaches 7 to 9 m depth (El'Ghmari, 1995) than springs with
401 high U AR. The spring BH, with the highest U AR is located at the bottom of the watershed where
402 the saprolite layer reaches less than 1.5 m thickness (Fig. 1). Also RUZS was taken at low altitude
403 (950masl), but drains the whole wetland and, therefore, integrated an intermediate U AR. Thus, a
404 possible scenario explaining the ($^{234}\text{U}/^{238}\text{U}$) AR of the spring waters is that BH like sources are
405 closer to the "fresh" granite and reflect meteoric alteration of fresher rock material at secular
406 equilibrium, CS₁, CS₃, CS₂, CS₄ and SH sources, by contrast, drain thicker saprolite profiles and/or
407 less fresh granite and, therefore, their low AR may point to the mobilization of U from mineral
408 phases whose outermost surfaces have already been depleted in ^{234}U due to previous water-rock
409 interactions (old saprolite where the pool of excess ^{234}U has been exhausted). We therefore propose
410 that the $^{234}\text{U}/^{238}\text{U}$ AR in the catchments spring waters can be interpreted as a function of water
411 pathways. The sources emerging at high altitude, with AR<1, have circulated through already
412 weathered horizons (saprolite, fractured bedrock depleted in ^{234}U , i.e., with U AR <<1), whereas the
413 springs emerging at the bottom of the watershed have U AR>1 because of the interaction with

414 fresher mineral phases. Therefore, U disequilibrium ratios can be a powerful tool to study the water
415 pathways. These preferential flow paths cross more or less weathered materials implying various
416 ($^{234}\text{U}/^{238}\text{U}$) AR for the corresponding springs.

417 This interpretation is in agreement with a granite leaching experiment under continuous flow
418 through a reactor (Andersen et al., 2009). It has indeed been shown that during the experiment
419 (1200 hours) there is a clear trend of variation of the U AR in the outflowing waters, with
420 ($^{234}\text{U}/^{238}\text{U}$) AR >1 at the beginning of the experiment and a minimal value of 0.9 after 650 to 700
421 hours; then, the AR increased up to 0.95. The values suggest that at the beginning of the experiment
422 high exposure of fresh material promotes direct recoil of ^{234}U into water and potentially enhances
423 preferential release of ^{234}U from damaged lattice sites. However, since there was no renewal of
424 material, because the excess ^{234}U constitutes a finite pool of easy leachable ^{234}U , the ($^{234}\text{U}/^{238}\text{U}$)
425 values become lower than unity when this pool is used up.

426 Similarly, the observed ($^{234}\text{U}/^{238}\text{U}$) AR <1 in Strengbach springs might indicate that the rate of
427 production of ^{234}U excess (by direct recoil and preferential release) is lower than the rate of renewal
428 of material. This can be explained by continuous preferential water circulation along fractures (Le
429 Borgne et al., 2007), on old weathered mineral surfaces where the production of ^{234}U excess is
430 supposed to be low.

431 However, the springs emerging at lower altitude (mainly BH and to a lesser extend RH), with
432 ($^{234}\text{U}/^{238}\text{U}$) >1, circulate through fresher granite where α -recoil tracks have direct contact with the
433 outer mineral surfaces and thus with fresh mineral phases (Andersen et al., 2009).

434 At this point it is interesting to note that in a neighbored granite catchment (Ringelbach watershed)
435 all the sources only display U AR >1 (Schaffhauser, 2013; Schaffhauser et al., 2014). This small
436 catchment located in the Vosges massif at altitudes between 750 and 1100m (0.36 km²) also
437 consists of Hercynian granite capped in its upper part by residual Triassic sandstones (Schaffhauser
438 et al., 2014).

439 Plotting the U AR of springs of the both watersheds versus alkalinity and pH (Fig. 10) one observes
440 a good correlation where springs with highest U AR are characterized by highest alkalinity and pH
441 values. These two parameters can be considered to reflect the intensity of weathering and
442 water/rock interactions, meaning that the waters from the Ringelbach watershed are characterized
443 by more intense weathering. Only SG spring from the Strengbach catchment shows a slightly
444 different behavior because it originates from a gneiss and not a granite body (see section 5.1). The
445 modeling of chemical composition of the waters from the Ringelbach catchment implies mainly
446 dissolution of primary granite minerals and precipitation of secondary phases such as clays
447 (Schaffauser, 2013). Ringelbach stream waters present higher alkalinity, pH (Fig. 10) and also
448 conductivity, K, Mg, Si and Ca concentrations (not show) than spring and stream waters from
449 Strengbach watershed, which might point to higher dissolution processes. Thus, we suggest that the
450 waters with the lowest U AR correspond to less intense weathering in an already rock altered
451 system with only a few fresh and primary mineral phases whereas higher U AR correspond to more
452 intense weathering for waters circulating for example in fresher bedrock. In this way, the
453 weathering history might be older for the Strengbach watershed than the Ringelbach watershed.
454 This may be related to the fact that Triassic sandstones still cover the granite in the Ringelbach
455 catchment.

456 It is striking that the BH waters from Strengbach watershed plot in between the data from the
457 Strengbach and Ringelbach watershed (Fig. 10a and b) and are characterized by the highest pH
458 (6.7) and alkalinity despite the relatively high DOC content (2.27 ppm), which usually increases the
459 acidity of solution. If we consider that the proton inputs due to atmospheric deposition or biological
460 activity are homogeneous at the watershed scale, then the variations of pH in the different springs
461 only reflect water/rock interactions and the consumption of protons by dissolution reactions. The
462 high pH and alkalinity observed for the BH source are in this case consistent with the fact that its
463 water has interacted with fresher bedrock; this further implies a stronger weathering intensity and
464 higher dissolution rate of secondary phases such as smectite along the pathway of this source water.

465 In such a scenario, the relationship observed between ($^{234}\text{U}/^{238}\text{U}$) AR and Mg/Ca ratios (Fig. 11)
466 would indicate that the intensity or the nature of water reactions controlling the Ca-Mg budget of
467 these waters, namely the dissolution/precipitation reactions of Mg- or Ca-smectites (see discussion
468 in 5.1), would be clearly dependent on the weathering level of the saprolite/bedrock system. This is
469 consistent with the fact that 1) smectite occurs along the weathering profile and even in deep
470 weathering horizons (Fichter et al., 1998) and 2) the reactivity of secondary phases like smectite
471 control the chemistry of Mg and Ca in streamwater (this study, Godderis et al., 2006; 2009). In
472 addition, dissolution of clays implies an increase of Mg/Ca ratios in water (Fig. 8b). Thus, the
473 relation between U AR and Mg/Ca ratios for the Strengbach springs reflects nothing else than the
474 degree of alteration of the source rock being in contact with the waters: at low altitude the material
475 is fresher, the weathering intensity is more important (higher pH and alkalinity) and, thus, causes
476 higher Mg/Ca and U AR ratios in the waters than at higher altitudes.

477

478 **5.3. Temporal variations of spring waters**

479 The data obtained during 2 hydrological years allow for the analysis of the temporal variations of
480 the springs (Fig. 3). The spring RUZS shows the largest variations, which can be explained by the
481 fact that this spring drains wetland (10 to 15 % of the whole catchment area) with fluctuations in the
482 groundwater level and contributions.

483 The Sr isotopic compositions of single springs are correlated with discharge (Fig. 6a). In previous
484 studies these variations have been interpreted by mixing of superficial (soil solution type) and deep
485 (groundwater type) waters (Aubert et al., 2002). But, at the same time, the U AR show no temporal
486 variation and, therefore, no relation with discharge (Fig. 6b).

487 Consequently, the U AR and Sr isotopic compositions are not correlated. Similarly, there is no
488 correlation between U AR and geographical location and lithology (discussed in section 5.2). In
489 addition, the lack of temporal U AR variations indicates that the single springs are probably not the
490 result of mixing of different waters. In the same way, the lack of correlation between discharge and

491 DOC or NO₃, but also the majority of major and trace element concentrations suggests that the
492 variation of chemical composition of spring waters cannot be explained by a simple variation in the
493 contribution between different types of waters or as mixing between superficial waters (with high
494 DOC, NO₃ concentrations for instance) and deep waters. At the same time, the lack of correlation
495 between Sr isotopic compositions and concentrations for individual springs (Fig. 4a) confirms that
496 the temporal variations of spring waters cannot simply be explained by mixing between two end-
497 members (e.g. superficial and deep waters). The lack of variation of U AR in the individual springs
498 with changing discharge (Fig. 6) during 2 years further suggests that the water pathways are the
499 same whatever the hydrological conditions. Under these conditions, the water did not interact with
500 new fresh material but rather with minerals having experienced at their surface a prior loss of ²³⁴U
501 from damaged lattice sites (Andersen et al., 2009). In such a fractured bedrock system, the water
502 flow is often reduced to only a few main flow paths that control most of the hydrological response
503 of the aquifer (Le Borgne et al., 2007). These preferential flow paths along constant fractures in the
504 bedrocks might explain the homogeneous (²³⁴U/²³⁸U) AR of the different spring waters with time.

505 In contrast, there is a correlation between discharge and ⁸⁷Sr/⁸⁶Sr ratios for each single spring (Fig.
506 6b). With increasing discharge the Sr isotopic composition increases as well, whereas the Si
507 concentrations and alkalinity decrease (Fig. 12).

508 Different Si concentration-discharge relationships have been observed in several catchments and
509 three different types have been identified: type 1 when Si concentration decreases with discharge;
510 type 2 when Si concentration remains constant and type 3 when Si concentration remains constant
511 until a threshold in discharge is exceeded (Godsey et al., 2009; Maher, 2011). The springs from the
512 Strengbach watershed belong to the type 1 which are explained by average residence times shorter
513 than required to approach chemical equilibrium. Thus, the chemistry of waters could vary entirely
514 as a function of the nature of subsurface flow paths and the global solute fluxes depend strongly on
515 the geometry, relief, runoff and permeability of basins (Maher, 2011). In addition, the variation of
516 the Sr isotopic compositions with discharge suggests that the source of Sr changes with changing

517 hydrological condition; this confirms again that the temporal variation cannot be explained by a
518 mixing process but possibly by changing residence times of fluid and/or flow rate which according
519 to Maher (2010) have an important impact on the weathering rates. This is in accordance with the
520 hypothesis of preferential flow pathways through fractures for the water circulation in the basin.
521 In addition, modeling studies have shown that precipitation/dissolution process of secondary phases
522 control the dissolved Si export in stream waters (Godderis et al., 2006; Violette et al., 2010;
523 Beaulieu et al., 2011). Thus, the decrease of Si concentration with increasing discharge can be
524 explained by a change in the ratio between dissolution and precipitation of clays (see also chapter
525 5.2). We propose that at high discharge the water is undersaturated for clay precipitation (lower Si
526 concentration) causing a more important contribution by dissolution of clays as implied by the
527 higher Mg/Ca (see chapter 5.1) and Sr isotopic ratios (Fig. 11c). Thus, our study confirms that
528 hydrological properties limit the solute fluxes carried by rivers and physico-chemical conditions.

529

530 **5.4. The chemical and isotopic signatures of the waters at the Strengbach outlet**

531 The stream at the catchments outlet shows with increasing discharge increasing $^{87}\text{Sr}/^{86}\text{Sr}$ and
532 decreasing alkalinity, pH, H_4SiO_4 , and $(^{234}\text{U}/^{238}\text{U})$ AR (Fig. 13a-e). The important point is that the
533 variation of U AR observed at the outlet (Fig. 13e) can only be explained by a change in the
534 discharge contribution of the different springs because the U AR of single springs are constant with
535 time (Fig. 6). When the discharge increases, the U AR values tend towards 0.95, which is close to
536 the $(^{234}\text{U}/^{238}\text{U})$ AR of the spring from the saturated area (RUZS) (Figs. 6 and 14). Previous papers
537 proposed that during storm events, the contribution of the small saturated zone could reach up to 30
538 % of the runoff (Idir et al., 1999; Ladouche et al., 2001). Similarly, the increase of the Sr isotopic
539 composition with increasing discharge points to the important contribution of RUZS to the
540 streamlet during high discharge events (Fig. 13d).

541 However, during the lowest discharge, the U AR of the stream at the outlet is > 1 (max. 1.023).

542 These higher values can only be explained by a more important contribution of the spring BH from

543 the northern slope which is the only one with a U AR>1 (average: 1.103; Table 1; Fig.14). Other
544 parameters such as H₄SiO₄, pH and alkalinity confirm the important contribution of the BH spring
545 to the streamlet during low discharge (Fig. 13). Similarly, the position of the RUZS spring with the
546 low pH, alkalinity and silica concentrations (Fig. 13) confirms its important contribution during
547 high discharge. But also the fact that the Sr isotopic composition of the stream at the outlet
548 decreases with decreasing discharge is in accordance with a more important contribution of the less
549 radiogenic springs from the northern (e.g. BH) (Fig. 13) than from the southern slope (Fig. 4).

550

551 **6. Conclusion :**

552 The study shows that the small Strengbach catchment drains different sources and streams with very
553 different isotopic and geochemical signatures. This heterogeneity is mainly related to:

554 - the parent material (gneiss, more or less hydrothermally altered granite) and the degree of their
555 weathering. This is confirmed by the fact that the sources draining the northern slope
556 (hydrothermally much more altered) have higher TDSw-, pH values, higher Ca, K, Mg
557 concentrations and lower ⁸⁷Sr/⁸⁶Sr ratios than sources draining the southern slope.

558 - the water flow is probably controlled by pathways through main fractures, as it is generally the
559 case in fractured granite systems.

560 This study has also shown, that there is an important decoupling between chemical composition on
561 the one hand and the ⁸⁷Sr/⁸⁶Sr ratios and (²³⁴U/²³⁸U) AR on the other hand. The Sr isotopic
562 compositions of the source waters are generally thought to be the result of alteration of primary
563 mineral phases such as apatite. However, the low apatite-like Sr isotopic composition but
564 comparatively high and not apatite-like Mg/Ca ratio cannot simply be derived from apatite
565 dissolution; however, they might originate from alteration of secondary mineral phases like clay
566 minerals, which integrated during their formation an apatite-derived Sr isotopic composition. The
567 dissolution and precipitation dynamics of secondary phases, especially clays such as
568 montmorillonite, seem to control the mobility of Si, Ca or Mg and, therefore, emphasize the key

569 role of the clays reactivity in the biogeochemical transfer of especially nutrient elements like Ca and
570 Mg.

571 Different processes control the variation of the U AR. Springs at high altitude with U AR<1 have
572 circulated through already weathered bedrock (thick saprolite and fractured rock) and have
573 interacted with already weathered surface minerals. These uncommon values for surface waters are
574 due to strong ^{234}U depletion during predating alteration processes of the bedrock granite. At the
575 opposite, springs emerging at the bottom of the watershed have U AR >1 because of interaction
576 with fresher materials.

577 The lack of variation of U AR in the individual springs with changing discharge during 2 years
578 suggests that the water pathways are the same whatever the hydrological conditions and that there is
579 no interaction between the different source waters.

580 It appears that the ($^{234}\text{U}/^{238}\text{U}$) AR is a very important tracer for studying and deciphering the
581 contribution of the different source fluxes at the catchment scale because this unique geochemical
582 parameter is different for each individual spring and at the same time remains unchanged for each
583 of the springs with changing discharge and fluctuating hydrological conditions. Without this
584 parameter it would not have been possible to decipher the real contribution of the different water
585 masses, especially that of the BH spring at low discharge conditions.

586 Thus all these observations converge toward the same functioning:

587 - The proportion of the contributions of the different springs to the stream at the outlet varies in
588 function of the hydrological conditions; the variable contributions of the different sources carrying
589 different geochemical signatures define the signature of the waters at the Strengbach outlet.

590 - During high flow events, the contribution of the saturated area (RUZS) to the streamlet increases.

591 - At low discharge, the contributions of springs from the northern slope become important (e.g.
592 BH).

593 The U-Sr isotope study, combined with physico-chemical investigations of the waters offered the
594 opportunity to better understand the processes causing the hydrochemical signature and its temporal

595 variation in each of the individual springs and in the stream waters at the outlet of the small
596 catchment. Indeed, this work points not only to the importance to investigate larger time intervals
597 including one total or even two hydrological cycles but also the interest of geographically enlarged
598 studies including several springs; punctual or only outlet observations will not allow for
599 understanding of the complex functioning of a watershed.

600 The study further highlights the important impact of different and independent water pathways in
601 fractured granite controlling the different geochemical and isotopic signatures of the waters.

602

603 **Acknowledgements**

604 We thank Daniel Million, Sophie Gangloff, Sylvain Bénarioumlil and René Boutin for technical
605 assistance. We would like to warmly acknowledge Yves Godd ris and Yann Lucas for discussion
606 about modeling. The manuscript benefit from constructive reviews from Stephan SK K hler and an
607 anonymous reviewer. The Observatoire Hydro-G ochimique de l'Environnement OHGE is
608 financially supported by INSU-CNRS, as well as by the REALISE network. This work has been
609 funding by EC2CO INSU CNRS program, and by 7th PCRD EU program (SoilTrec program). This
610 is an EOST contribution.

611

612

613 **References:**

614

615 Andersen M.B., Erel Y. and Bourdon B.: Experimental evidence for ^{234}U - ^{238}U fractionation during
616 granite weathering with implications for $^{234}\text{U}/^{238}\text{U}$ in natural waters. *Geochim. Cosmochim. Ac.*, 73.
617 4124-4141. 2009.

618 Andrews J.N. and Kay R.L.F.: The U contents and $^{234}\text{U}/^{238}\text{U}$ activity ratios of dissolved uranium in
619 groundwaters from some Triassic sandstones in England. *Isotope Geoscience* 1. 101-117. 1983.

620 Aubert D., Stille P. and Probst A.: REE fractionation during granite weathering and removal by
621 waters and suspended loads: Sr and Nd isotopic evidence. *Geochim. Cosmochim. Ac.* 65. 387-406.
622 2001.

623 Aubert D., Probst A., Stille P. and Viville D.: Evidence of hydrological control of Sr behavior in
624 stream water (Strengbach catchment, Vosges mountains, France). *Appl. Geochem.*, 17. 285-300.
625 2002.

626 Bagard M.L., Chabaux F., Pokrovsky O.S., Viers J., Prokushkin A.A., Stille P., Rihs S., Schmitt
627 A.D. and Dupré B.: Seasonal variability of element fluxes in two Central Siberian rivers draining
628 high latitude permafrost dominated areas. *Geochim. Cosmochim. Ac.*, 75. 3335-3357. 2011.

629 Berger T.W., Untersteiner H., Schume H. and Jost G.: Throughfall fluxes in a secondary spruce
630 (*Picea abies*), a beech (*Fagus sylvatica*) and a mixed spruce-beech stand. *For. Ecol. Manage.*, 255.
631 605-618. 2008.

632 Beaulieu E., Godderis Y., Labat D., Roelandt C., Calmels D. and Gaillardet J.: Modeling of water-
633 rock interaction in the Mackenzie basin: Competition between sulfuric and carbonic acids. *Chem.*
634 *Geol.*, 289. 114-123. 2011.

635 Bickle M.J., Chapman H.J., Bunbury J., Harris N.B.W., Fairchild I.J., Ahmad T. and Pomies C.:
636 Relative contributions of silicate and carbonate rocks to riverine Sr fluxes in the headwaters of the
637 Ganges. *Geochim. Cosmochim. Ac.*, 69. 2221-2240. 2005.

638 Blum J.D., Carey A.G., Jacobson A.D., and Chamberlain P.: Carbonate versus silicate weathering
639 in the Raikhot watershed within the High Himalayan Crystalline Series. *Geology*. 26. 411–414.
640 1998.

641 Blundy J. and Wood B.: Mineral-melt partitioning of uranium, thorium and their daughters. In :
642 *Uranium-Series Geochemistry*. 52. 59-123. 2003.

643 Bonotto D. M. and Andrews J. N.: The mechanism of U-²³⁴/U-²³⁸ activity ratio enhancement in
644 karstic limestone groundwater. *Chem. Geol.*. 103. 193–206. 1993.

645 Bonotto D.M., Andrews J.N.: The transfer of uranium isotopes ²³⁴U and ²³⁸U to the waters
646 interacting with carbonates from Mendip Hills area (England). *Appl. Radiat. Isotopes*. 52. 965-983.
647 2000.

648 Bourdon B., Bureau S., Andersen M.B., Pili E. and Hubert E.: Weathering rates from up to bottom
649 in carbonate environment. *Chem. Geol.*. 258. 275-287. 2009.

650 Boutin R., Montigny R. et Thuizat R.: Chronologie K-Ar et ³⁹Ar/⁴⁰Ar du métamorphisme et du
651 magmatisme des Vosges. Comparaison avec les massifs varisques avoisinants et détermination de
652 l'âge de la limite Viséen inférieur – viséen supérieur. *Geologie de la France* 1. 3-25. 1995.

653 Brantley S.L., Goldhaber M.B. and Ragnarsdottir V. K.: Crossing disciplines and scales to
654 understand the Critical Zone. *Elements*. 3. 307-314. 2008.

655 Brioshi L., Steinmann M., Lucot E., Pierret M.C., Stille P., Prunier J. and Badot P.M. : Transfer of
656 rare earth elements (REE) from natural soil to plant systems: implications for the environmental
657 availability of anthropogenic REE. *Plant Soil*. 366. 143-163. 2013.

658 Camacho A., Devesa R., Vallés I., Serrano I., Soler J., Blasquez S., Ortega X. and Matia L.:
659 Distribution of uranium isotopes in surface water of the Llobregat river basin (Northeast Spain). *J.*
660 *Environ. Radioactiv.*. 101. 1048-1054. 2010

661 Cenk Tok B., Chabaux F., Lemarchand D., Schmitt A.-D., Pierret M.-C., Viville D., Bagard M.-
662 L. and Stille P.: The impact of water-rock interaction and vegetation on calcium isotope

663 fractionation in soil- and stream waters of a small. forested catchment (the Strengbach case).
664 *Geochim. Cosmochim. Ac.*. 73. 2215-2228. 2009.

665 Chabaux. F.. O'Nions. R.K.. Cohen. A.S.. Hein J.R.: ^{238}U - ^{234}U - ^{230}Th disequilibrium in Fe-Mn crusts :
666 Palaeoceanographic record or diagenetic alteration? *Geochim. Cosmoch. Ac.*. 61.. 3619-3632. 1997.

667 Chabaux. F.. Riotte. J.. Clauer. N. and France-Lanord. C.: Isotopic tracing of the dissolved U
668 fluxes in Himalayan rivers: implications for present and past U budgets of the Ganges-Brahmaputra
669 system *Geochim. Cosmoch. Ac.*. 65. 3201-3217. 2001.

670 Chabaux F.. Riotte J.. Dequincey O.: U-Th-Ra fractionation during weathering and river transport.
671 *Rev. Mineral. Geochem.*. 52. 533-576. 2003.

672 Chabaux. F.. Riotte. J.. Schmitt. A.-D.. Carignan. J.. Herckes. P.. Pierret. M.-C.: Variations of U
673 and Sr isotope ratios in Alsace and Luxembourg rain waters: origin and hydrogeochemical
674 implications. *C. R. Geosci.*. 337. 1447-1456. 2005.

675 Chabaux. F.. Bourdon. B.. Riotte. J.: U-series Geochemistry in weathering profiles. river waters and
676 lakes. In : S. Krishnaswami and J.K. Cochran (Eds.). *U/Th Series Radionuclides in Aquatic
677 Systems*. Elsevier. Amsterdam. *Radioactivity in the Environment*. 13. 49-104. 2008.

678 Chabaux F.. Granet M.. Larque P.. Riotte J.. Skliarov E.V.. Skliarova O.. Alexeieva L.. Risacher F.:
679 Geochemical and isotopic (Sr. U) variations of lake waters in the Ol'khon Region. Siberia. Russia:
680 Origin and paleoenvironmental implications. *C.R. Geosci.*. 343. 462-470. 2011.

681 Chen J.H.. Edwards G.J. Wasserburg R.L.: ^{238}U - ^{234}U - ^{232}Th in seawater. *Earth Planet. Sci. Lett.*. 80.
682 241-251. 1986.

683 Cividini D.. Lemarchand D.. Boutin R.. Pierret M-C.. and Chabaux F.: From biological to
684 lithological control of the B geochemical cycle in a forested watershed (Strengbach. Vosges).
685 *Geochim. et Cosmochim. Ac.*. 74. 3143-3163. 2010.

686 Dambrine E.. Le Goaster S.. and Ranger J.: Croissance et nutrition minérale d'un peuplement
687 d'épicéa sur sol pauvre. II Prélèvement racinaire et transferts internes d'éléments minéraux au cours
688 de la croissance. *Ac. Œcol.*. 12. 791-808. 1991.

689 Dambrine E., Carisey N., Pollier B., and Granier A.: Effects of drought on the yellowing status and
690 the dynamic of mineral elements in the xylem sap of a declining spruce stand (*Picea abies* Karst.).
691 *Plant Soil*. 150. 303-306. 1992a.

692 Dambrine E., Pollier B., Poszwa A., Ranger J., Probst A., Viville D., Biron P. and Granier A.:
693 Evidence of current soil acidification in spruce (Strengbach catchment, Vosges mountains, North-
694 Eastern France). *Water, Air Soil Poll.*, 105. 43-52. 1992b.

695 Degens E.T., Kempe S. and Richey J.E.: *Biogeochemistry of Major World Rivers*. Wiley, New
696 York. 356 pp., 1991.

697 DePaolo D., Maher K., Christensen J.N. and McManus J.: Sediment transport time measured with
698 U-series isotopes: Results from ODP North Atlantic drift site 984. *Earth and Planetary Science*
699 *Letters*. 248. 394-410. 2006.

700 DePaolo D., Lee V.E., Christensen J.N., and Maher K.: Uranium comminution ages: Sediment
701 transport and deposition time scales. *C.R. Geosci.*, 344. 678-687. 2012.

702 Dosseto A., Bourdon B. and Turner S. P. : Uranium-series isotopes in river materials: insights into
703 the timescales of erosion and sediment transport. *Earth Planet. Sci Lett.*, 265(1-2). 1-17. 2008.

704 Dosseto A., Buss H., Suresh P.O. : Rapid regolith formation over volcanic bedrock and implications
705 for landscape evolution. *Earth Planet. Sc. Lett.*, 337-338. 47-55. 2012.

706 Dupré B., Dessert C., Oliva P., Goddérés Y., Viers J., François L., Millot R. and Gaillardet J.:
707 Rivers, chemical weathering and Earth's climate. *C.R. Geosciences*. 335. 1141-1160. 2003.

708 Durand S., Chabaux F., Rihs S., Düringer P. and Elsass P.: U isotope ratios as tracers of
709 groundwater inputs into surface waters: example of the Upper Rhine hydrosystem. *Chem. Geol.*,
710 220. 1-19. 2005.

711 Egli. M., Mirabella. A., Sartori. G., Giaccari. D., Zanelli. R. & Plötze. M. : Effect of slope aspect on
712 transformation of clay minerals in Alpine soils. *Clay Minerals*. 42. 375-401. 2007.

713 Egli. M.. Sartori. G. and Mirabella. A. : The effects of exposure and climate on the weathering of
714 late Pleistocene and Holocene Alpine soils. *Geomorph.* 114. 466-482. 2010

715 El Gh'Mari A.: Etude minéralogique. pétrophysique et géochimique de la dynamique d'altération
716 d'un granite soumis au dépôts atmosphériques acides (Bassin versant du Strengbach. Vosges.
717 France) mécanismes. bilans et modélisations. PhD. Thesis. University Strasbourg. 202 p.. 1995.

718 Engstrom E.. Rodushkin I.. Ingri J.. Baxter D.C. Ecke F.. Osterlund H. and Ohlander B.: Temporal
719 isotopic variations of dissolved silicon in a pristine boreal river. *Chem. Geol.* 271. 142-152. 2010.

720 Fichter J.: Minéralogie quantitative et flux d'éléments minéraux libéré par altération des minéraux
721 des sols dans deux écosystèmes sur granite (Bassin versant du Strengbach. Vosges). PhD thesis.
722 Univ. Henri Poincaré. Nancy I. 284 p.. 1997.

723 Fichter J.. Turpault M.P.. Dambrine E.. and Ranger J.: Mineral evolution of acid forest soils in the
724 Strengbach catchment (Vosges mountains. N-E France). *Geoderma*. 82. 315-340. 1998.

725 Gaillardet J.. Dupré B.. Louvat P.. and Allègre C.J.: Global silicate weathering and CO₂
726 consumption rates deduced from the chemistry of the large rivers. *Chem. Geol.* 159. 3-30. 1999.

727 Goddérès Y.. François L.M.. Probst A.. Schott J.. Moncoulon D.. Labat D. and Viville D.:
728 Modelling weathering processes at the catchment scale: The WITCH numerical model. *Geochim.*
729 *Cosmochim. Ac.* 70. 1128-1147. 2006.

730 Goddérès Y.. Roelandt C.. Schott J.. Pierret M.C. and François L.: Towards an integrated model of
731 weathering. climate. and biospheric processes. *Rev. Mineral. Geochem.* 70. 411-434. 2009.

732 Godsey S.E.. Kirchner J.W.. Clow D.W.: Concentration-discharge relationships reflect chemostatic
733 characteristics of US catchments. *Hydrol. Process.* 23. 1844-1864. 2009.

734 Grzymko T.J.. Marcantonio F.. McKee B.A. and Stewart C.M.: Temporal variability of uranium
735 concentrations and ²³⁴U/²³⁸U activity ratios in the Mississippi river and its tributaries. *Chem. Geol.*
736 243. 344–356. 2007.

737 Hindshaw R.S.. Tipper E.T.. Reynolds B.C.. Lemarchand E.. Wiederhold J.G.. Magnusson J..
738 Bernasconi S.M.. Kertzschar R.. and Bourdon B.: Hydrological control of stream water chemistry

739 in a glacial catchment (Damma Glacier, Switzerland). *Chem. Geol.*, 285, 215–230. 2011.

740 Idir S., Probst A., Viville D. and Probst J.L.: Contribution des surfaces saturées et des versants aux
741 flux d'eau et d'éléments exportés en période de crue : tracage à l'aide du carbone organique dissous
742 et de la silice. Cas du petit bassin versant du Strengbach (Vosges, France). *C.R. Acad. Sci.*, 328, 89-
743 96. 1999.

744 Kohler S.J., Lidman F. and Laudon H. : Landscape types and pH control organic matter mediated
745 mobilization of Al, Fe, U and La in boreal catchments. *Geochim. Cosmochim. Acta.*, 135, 190-202.
746 2014.

747 Ladouche B., Probst A., Viville D., Idir S., Baqué D., Loubet M., Probst J.-L., and Bariac T.:
748 Hydrograph separation using isotopic, chemical and hydrological approaches (Strengbach
749 catchment, France). *J. Hydrol.*, 242, 255-274. 2001.

750 Lahd Geagea M., Stille P., Gauthier-Lafaye F. and Millet M.: Tracing of industrial aerosol sources
751 in an urban environment using Pb, Sr and Nd isotopes. *Env. Sci. and Technol.*, 42, 692-698. 2008a.

752 Lahd Geagea M., Stille P., Gauthier-Lafaye F., Perrone T. and Aubert D.: Baseline determination of
753 the atmospheric Pb, Sr and Nd isotopic composition of the Rhine Valley, Vosges Mountain
754 (France) and the Central Swiss Alps. *Appl. Geochim.*, 23, 1703-1714. 2008b.

755 Laudon H., Seibert J., Kohler S. and Bishop K. : Hydrological flow paths during snowmelt:
756 congruence between hydrometric measurements and oxygen 18 in meltwater, soil water, and runoff.
757 *Water Resour. Res.*, 40, 3102–3102. 2004.

758 Le Borgne T., Bour O., Riley M.S., Gouze P., Pezard P., Belghoul A., Lods G., Le Provost R.,
759 Greswell R.B., Ellis P.A., Isakov E. and Last B.J.: Comparison of alternative methodologies for
760 identifying and characterizing preferential flow paths in heterogeneous aquifers. *J. Hydrol.*, 345,
761 134-148. 2007.

762 Lefèvre Y.: Les sols du bassin d'Aubure. (Haut-Rhin): caractérisation et facteurs de répartition.
763 *Ann. Sci. For.*, 45, 417-422. 1988.

764 Lemarchand E., Chabaux F., Vigier N., Millot R., Pierret M.C. : Lithium isotopic behaviour in a
765 forested granitic catchment (Strengbach, Vosges Mountains, France). *Geochim. Cosmochim. Ac.*,
766 74, 4612-4628. 2010.

767 Lemarchand D., Cividini D., Turpault M.P., Chabaux F. : Boron isotopes in different grain size
768 fractions : Exploring past and present water-rock interaction from two soil profiles (Strengbach,
769 Vosges Mountain). *Geochim. Cosmochim. Ac.*, 98, 78-93. 2012.

770 Maher K., Steefel C.I., DePaolo D.J. and Viani B.E. : The mineral dissolution rate conundrum:
771 Insights from reactive transport modeling of U isotopes and pore fluid chemistry in marine
772 sediments. *Geochim. Cosmochim. Ac.*, 70, 337–363. 2006.

773 Maher K. : The dependence of chemical weathering rates on fluid residence time. *Earth and*
774 *Planetary Science Letters*, 294, 101-110. 2010.

775 Maher K. : The role of fluid residence time and topographic scale in determining chemical fluxes
776 from landscapes. *Earth and Planet. Sc. Lett.*, 312, 48-58. 2011.

777 Martin J.M. and Meybeck M. : Element mass-balance of material carried by major world rivers.
778 *Mar. Chem.*, 7, 173-206. 1979.

779 Millot R., Gaillardet J., Dupré B. and Allègre C.J.: Northern latitude chemical weathering rates:
780 Clues from the Mackenzie River Basin, Canada. *Geochim. Cosmochim. Ac.*, 67, 1305–1329. 2003.

781 Négrel P., Allègre C.J., Dupré B., and Lewin E.: Erosion sources determined by inversion of major
782 and trace element ratios in river water: the Congo Basin case. *Earth Planet. Sci. Lett.*, 20, 59-76.
783 1993.

784 Oliva P., Viers J., and Dupré B.: Chemical weathering in granitic environments. *Chem. Geol.*, 202,
785 225-256. 2003.

786 Osmond J.K. and Cowart J.B.: The theory and uses of natural uranium isotopic variations in
787 hydrology. *Atomic Energy Rev.*, 14:621-679. 1976.

788 Osmond J.K., Cowart J.B.: Groundwater. In: *Uranium series disequilibrium – Applications to*
789 *environmental problems*. Ivanovich M. Harmon RS (eds) Oxford Science Publications, Oxford, p

790 202-245. 1982.

791 Osmond. J.K.. Ivanovich. M.: Uranium-series mobilisation and surface hydrology. In: Ivanovich.
792 M.. Harmon. R.S. (Eds.). Uranium-series Disequilibrium: Applications to Earth. Marine and
793 Environmental Sciences. second ed. Clarendon Press Oxford. 258-289. 1992.

794 Oster J.L.. Ibarra D.E.. Harris C.R. and Maher K.: Influence of eolian deposition and rainfall
795 amounts on the U-isotopic composition of soil water and soil minerals. Geochim. Cosmochim. Ac..
796 88. 146-166. 2012.

797 Paces J.B.. Ludwig K.R.. Peterman Z.E.. Neymark L.A.: $^{234}\text{U}/^{238}\text{U}$ evidence for local recharge and
798 patterns of ground-water flow in the vicinity of Yucca Mountain. Nevada. USA. Appl. Geochem..
799 17. 751-779. 2002.

800 Pelt E.. Chabaux F.. Innocent C.. Navarre-Sitchler A.L.. Sak P.B. and Brantley S.L.: Uranium-
801 thorium chronometry of weathering rinds: Rock alteration rate and paleo-isotopic record of
802 weathering fluids. Earth Planet. Sci. Lett.. 276. 98-105. 2008.

803 Pierret M.C.. Chabaux F.. Leroy S. and Causse C.: A record of Late Quaternary continental
804 weathering in the sediment of the Caspian Sea: evidence from U-Th. Sr isotopes. trace element and
805 palynological data. Quaternary Sci. Rev.. 51. 40-55. DOI 10. 1016/j.quascirev.2012.07.020. 2012.

806 Pierret M.C.. Bosch D.. Clauer N. and Blanc G.: Formation of metal-rich sediments in the Thetis
807 Deep (Red Sea) in the absence of brines : Implications for the genetic model. J. Geoch. Explor..
808 104. 12-26. DOI 10.1016/j.gexplo. 2009.

809 Probst A.. Dambrine E.. Viville D. and Fritz B.: Influence of acid atmospheric inputs on surface
810 water chemistry and mineral fluxes in a declining spruce stand within a small granitic catchment
811 (vosges massif- France). J. Hydrol.. 116. 101-124. 1990.

812 Probst A. Viville D. Fritz B. Ambroise B. and Dambrine E.: Hydrochemical budgets of a small
813 forested catchment exposed to acid deposition : the Strengbach catchment case study (Vosges
814 massif. France) W.A.S.P. 62. 337-347. 1992a.

815 Probst A., Fritz B., and Stille P.: Consequence of acid deposition on natural weathering processes:
816 field studies and modelling. In: Water Rock Interaction (Eds. Kharaka Y.K. and Maest A.S.)
817 Balkema/Rotterdam/ Brookfield. 581-584. 1992b.

818 Prunier J.: Etude du fonctionnement d'un écosystème forestier en climat tempéré. par l'apport de la
819 géochimie élémentaire et isotopique (Sr, U-Th-Ra). Cas du bassin versant du Strengbach (Vosges,
820 France). Thesis PhD. Uni. de Strasbourg. 303pp.. 2008.

821 Riotte J. and Chabaux F.: ($^{234}\text{U}/^{238}\text{U}$) activity ratios in freshwaters as tracers of hydrological
822 processes: the Strengbach watershed, Vosges, France. *Geochim. Cosmochim. Ac.*, 63, 1263-1275.
823 1999.

824 Riotte J., Chabaux F., Benedetti M., Dia A., Gérard M., Boulègue J., and Etamé J.: U colloidal
825 transport and origin of the ^{234}U - ^{238}U fractionation in surface waters : new insights from Mount
826 Cameroon. *Chem. Geol.*, 202, 365-381. 2003.

827 Schaffhauser T.: Traçage et modélisation des processus d'altération à l'échelle d'un petit bassin
828 versant, le Ringelbach (Vosges, France). Thesis PhD. Université de Strasbourg. 343pp. 2013.

829 Schaffhauser T., Chabaux F., Ambroise B., Lucas Y., Stille P., Perronne T., Fritz B.: Geochemical
830 and isotopic (U, Sr) tracing of water pathways in the small granitic Ringelbach research catchment
831 (Vosges Mountains, France). *Chem. Geol.*, 374, 117-127. 2014.

832 Steinmann M. and Stille P.: Controls on transport and fractionation of the rare earth elements in
833 stream water of a mixed basaltic-granitic catchment basin (Massif Central, France) *Chem. Geol.*,
834 254, 1-18. 2009.

835 Stille P., Steinmann M., Pierret M.-C., Gauthier-Lafaye F., Chabaux F., Viville D., Pourcelot L.,
836 Matera V., Aouad G., and Aubert D.: The impact of vegetation on REE fractionation in stream
837 waters of a small forested catchment (the Strengbach case). *Geochim. Cosmochim. Ac.*, 70, 3217-
838 3230. 2006.

839 Stille P., Pierret M.-C., Steinmann M., Chabaux F., Boutin R., Aubert D., Pourcelot L., and Morvan

840 G.: Impact of atmospheric deposition. biogeochemical cycling and water-mineral interaction on
841 REE fractionation in acidic surface soils and soil water (the; Strengbach case). *Chem. Geol.* 264.
842 173-186. 2009.

843 Stille P., Pourcelot L., Granet M., Pierret M.-C., Perrone Th., Morvan G. and Chabaux F. :
844 Deposition and migration of atmospheric Pb in soils from a forested silicate catchment today and in
845 the past (Strengbach case ; Vosges mountains) ; evidence from ^{210}Pb activities and Pb isotope
846 ratios. *Chem. Geol.* 289. 140-153. 2011.

847 Stille P., Schmitt A.-D., Labolle F., Gangloff S., Cobert F., Lucot E., Pierret M.-C., Guéguen F.,
848 Brioschi L., Steinmann M., Chabaux F. : The suitability of annual growth rings as environmental
849 archives: Evidence from Sr, Nd, Pb and Ca isotopes in spruce growth rings (Strengbach case;
850 Vosges mountains, France). *CR Geosci.* 344. 297-311. 2012.

851 Stromman G., Rosseland B.O., Skipperud L., Burbkitbaev L.M., Uralbekov B., Heier L.S., Salbu
852 B.: Uranium activity ratio in water and fish from pit lakes in Kurday, Kazakhstan and Taboshar,
853 Tajikistan. *J. Environ. Radioactiv.* 1. 11. 2012.

854 Tipper E.T., Bickle M.J., Galy A., West A. J., Pomies C., and Chapman H.J.: The short term
855 climatic sensitivity of carbonate and silicate weathering fluxes: Insight from seasonal variations in
856 river chemistry. *Geochim. Cosmochim. Ac.* 70. 2337-2754. 2006.

857 Tricca A., Stille P., Steinmann M., Kiefel B., Samuel, J., and Eikenberg J. : Rare earth elements and
858 Sr and Nd isotopic compositions of dissolved and suspended loads from small river systems in the
859 Vosges mountains (France), the river Rhine and the groundwater. *Chem. Geol.* 160. 139-158. 1999.

860 Thimonier A., Schmitt M., Waldner P., and Schleppe P.: Seasonality of the Na/Cl ratio in
861 precipitation and implication of canopy leaching in validating chemical analyses of throughfall
862 samples. *Atmos. Environ.* 42. 9106-9117. 2008.

863 Ulrich, B.: Interaction of forest canopies with atmospheric constituents: SO_2 , alkali and earth alkali
864 cations and chloride. In: Ulrich, B., Pankrath, J. (Eds.). *Effects of Accumulation of Air Pollutants in*
865 *Forest Ecosystems*. Reidel, Dordrecht. pp. 33–45. 1983.

866 Vigier N., Bourdon B., Turner S., and Allègre C.J.: Erosion timescales derived from U-decay series
867 measurements in rivers. *Earth Planet. Sci. Lett.*, 193, 549-563, 2001.

868 Vigier N., Burton K.W., Gilslason S.R., Rogers N.W., Duchon S., Thomas L., Hodge E., Schaefer
869 B.: The relationship between riverine U-series disequilibria and erosion rates in a basaltic terrain.
870 *Earth Planet. Sci. Lett.*, 249, 258-273, 2006.

871 Violette A., Godderis Y., Maréchal J.C., Riotte J., Oliva P., Mohan Kuma M.S., Sekhar M. and
872 Braun J.J. : Modelling the chemical weathering fluxes at the watershed scale in the Tropics (Mule
873 Hole, South India) : Relative contribution of the smectite/kaolinite assemblage versus primary
874 minerals. *Chem. Geol.*, 277, 42-60, 2010.

875 Viville D., Chabaux F., Stille P., Pierret M.C., Gangloff S.: Erosion and weathering fluxes in
876 granitic basins: The example of the Strengbach catchment (Vosges massif, eastern France). *Catena*,
877 92, 122-129, 2012.

878 Zakharova E.A., Pokrovsky O.S., Dupré B., Gaillardet J., Efimova L.E.: Chemical weathering of
879 silicate rocks in Karelia region and Kola peninsula, NW Russia: Assessing the effect of rock
880 composition, wetlands and vegetation. *Chem. Geol.*, 242, 255–277, 2007.

881

882

883

884

885

886

888

889 Table 1: Chemical compositions of spring and stream waters, open field precipitation, throughfalls
890 under spruces (PL5) and beeches (PLH). The total dissolved solids (TDS_w) have been calculated
891 from the major dissolved elements concentrations (cations, anions and silica) and are expressed in
892 mg/L. as calculated for several watersheds (e.g.. Gaillardet et al., 1999). Another parameter, called
893 here $TDS-Ca$ ($=Ca+Mg+Na+K+SiO_2+Fe$) has been calculated as proposed by Zakharova et al.
894 (2007) and reflects the silicate weathering.

895

896

Samples	date	⁸⁷ Sr/ ⁸⁶ Sr	2sigma	²³⁴ U/ ²³⁸ U	2sigma	altitude (m)
Spring CS1	28/09/04	0.72573	0.00002	0.880	0.001	1080
CS1	13/12/04	0.72656	0.00004	0.875	0.005	1080
CS1	29/03/05	0.72780	0.00001	0.892	0.003	1080
CS1	22/05/06	0.72650	0.00001	0.886	0.002	1080
CS1	Average	0.72665		0.883		
Spring CS2	03/05/05	0.72546	0.00001			1055
CS2	11/07/05	0.72376	0.00001			1055
CS2	22/05/06	0.72544	0.00001	0.875		1055
CS2	02/10/06	0.72515	0.00001			1055
CS2	Average	0.72495		0.875		
Spring CS3	13/12/04	0.72325	0.00002	0.823	0.003	1098
CS3	29/03/05	0.72328	0.00001	0.827	0.003	1098
CS3	11/07/05	0.72314	0.00002			1098
CS3	22/05/06	0.72325	0.00001	0.819	0.004	1098
CS3	Average	0.72323		0.823		
Spring CS4	03/05/05	0.72490	0.00002	0.866	0.003	1050
CS4	11/07/05	0.72375	0.00001			1050
CS4	22/05/06	0.72353	0.00001	0.867	0.002	1050
CS4	02/10/06	0.72548	0.00001			1050
CS4	Average	0.72442		0.867		
Spring BH	12/07/04	0.72262	0.00002	1.106	0.005	915
BH	13/12/04	0.72289	0.00002	1.1	0.003	915
BH	29/03/05	0.72359	0.00001	1.101	0.003	915
BH	03/05/05	0.72340	0.00001	1.1	0.003	915
BH	31/05/05	0.72319	0.00001	1.112	0.003	915
BH	11/07/05	0.72279	0.00001	1.101	0.003	915
BH	22/08/05	0.72287	0.00001	1.106	0.003	915
BH	03/10/05	0.72307	0.00001	1.105	0.003	915
BH	22/05/06	0.72334	0.00002	1.099	0.004	915
BH	Average	0.723084		1.103		
Spring RUZS	13/12/04	0.72700	0.00002	0.945	0.004	950
RUZS	29/03/05	0.72665	0.00001	0.941	0.003	950
RUZS	22/05/06	0.72669	0.00001	0.949	0.003	950
RUZS	Average	0.72678		0.945		
Spring RH	28/09/04	0.72206	0.00008	0.996	0.003	980
RH	13/12/04	0.72240	0.00002	0.991	0.004	980
RH	29/03/05	0.72257	0.00002	0.993	0.005	980
RH	22/05/06	0.72242	0.00001	0.991	0.004	980
RH	Average	0.72236		0.993		
Spring SG	28/09/04	0.72353	0.00002	0.91	0.004	1093
SG	13/12/04	0.72328	0.00007	0.93	0.003	1093
SG	29/03/05	0.72352	0.00002	0.923	0.004	1093
SG	22/05/06	0.72354	0.00002	0.927	0.002	1093
SG	Average	0.72347		0.923		
Spring SH	28/09/04	0.72749	0.00003	0.916	0.003	1050
SH	13/12/04	0.72720	0.00009	0.915	0.003	1050
SH	29/03/05	0.72801	0.00002	0.914	0.004	1050
SH	03/05/05	0.72798	0.00001			1050
SH	22/05/06	0.72720	0.00001	0.911	0.004	1050
SH	02/10/06	0.72752	0.00001			1050
SH	Average	0.72757		0.914		
Outlet RS	29/03/05	0.72573	0.00002	0.939	0.003	883
RS	22/05/06	0.72520	0.00001	0.974	0.004	883
RS	Average	0.72547		0.957		
atmospheric inputs	Average					
Rain	2004-2006	0.7111		1.175		
Throughfalls spruces	2004-2006	0.71290		1.079		
Throughfalls beeches	2004-2006	0.71620		0.953		
clays SS under beeches	35 cm depth	0.872847	0.00002	1.26	0.003	
clays SS under beeches	95 cm depth	0.767439	0.00001	1.074	0.002	
clays NS under spruces	35 cm depth	0.830034	0.00001	1.094	0.002	
clays NS under spruces	95 cm depth	0.802886	0.00001	nd		

897

898 Table 2: Sr isotopic compositions and U AR for spring waters, outlet, rain, throughfalls and clays
899 (Prunier, 2008) from the Strengbach watershed. Clays SS: clays from a soil profile located on the
900 southern slope and under beeches, and clays NS: clays from a soil profile located on the northern
901 slope and under spruces.

902

2004-2006	water fluxes (mm)	Na fluxes mg/m ² /yr	K fluxes mg/m ² /yr	Mg fluxes mg/m ² /yr	Ca fluxes mg/m ² /yr	Si fluxes mg/m ² /yr	Sr fluxes µg/m ² /yr	U fluxes µg/m ² /yr
rain - F _{rain}	1247	306	219	56	256	5	1.1	7.6
throughfall - F _{throughfall}	1070	1041	3037	256	1034	101	2.4	12.6
biological contribution to throughfalls C _b (1.2.3.4)		0.2	0.9	0.3	0.25	0.1	nd	nd
Atmospheric contribution to throughfall - F _{throughfall(corrected)}		833	304	179	776	91	nd	nd
global atmospheric input (a)	1096	754	291	161	697	78	1.1 to 2.4	7.6 to 12.6
outlet fluxes (b)	850	1634	608	456	2276	3008	8.8	113
rain-corrected outlet fluxes (c)	850	1328	388	399	2019	3003	7.7	105
(wet+dry atmos. deposits)-corrected outlet fluxes (d)	850	880	317	295	1579	2929	7.7 to 6.6	105 to 101

903

904 Table 3: Elementary fluxes for rain, throughfalls and outlet in the Strengbach catchment. The rain
 905 corresponds to open field precipitations, the throughfalls have been collected under spruces (80% of
 906 the forest cover) and beeches (20% of the forest cover). The chemical composition of throughfalls
 907 includes wet and dry atmospheric deposition and biological excretion (biological leaching). In order
 908 to estimate the atmosphere-derived fluxes (input fluxes) we applied for every element a specific
 909 corrective factor C_b (1) Ulrich et al. 1983; (2) Dambrine et al., 1998; (3) Thimonier et al., 2008. (4)
 910 Berger et al., 2008. The global atmospheric input has been calculated considering the catchment
 911 area as 15% of clearing and 85% of forest, the formula is then: $F_{atm} = 0.15 F_{rain} + 0.85 F_{throughfall(corrected)}$.

912 The outlet fluxes correspond to the catchment export fluxes (b).

913

914

915

916

917

918

919

920

Soils under spruces - Northern slope (1)																									
depth	SiO2	Al2O3	MgO	CaO	Fe2O3	MnO	TiO2	Na2O	K2O	P2O5	Mg/Ca	Mg/Na	Ca/Na	muscovite	Quartz	K-Feld	plagio	apatite	Smectite	amorph	smectite (%)	OM	pH	Clays	CEC
cm	%	%	%	%	%	%	%	%	%	%	%	%	%	%	%	%	%	%	%	%	in clay fract.	%		%<2µm	cmol/kg
10	72.74	17.84	0.51	0.06	1.92	0.04	0.24	0.62	5.70	0.22	7.56	1.34	0.18	42.2	38.6	10.9	5.4	0.05	3.7	0.68	19.7	7.5	3.7	22.2	15.49
50	64.82	20.71	0.66	0.15	2.43	0.04	0.32	0.85	5.60	0.43	3.65	1.27	0.35	50.1	27.3	5.6	7.5	0.21	5.8	1.09	19.8	9.2	4.4	20.3	11.98
70	65.89	20.59	0.65	0.28	2.12	0.03	0.22	0.99	5.99	0.52	1.95	1.07	0.55	47.5	27.8	7	8.7	0.42	6	1.11		7	4.4	15.8	10.37
90	68.10	20.44	0.70	0.28	2.04	0.02	0.20	0.92	5.71	0.43	2.10	1.24	0.59	45.4	27.4	8.9	8.1	0.43	7.8	0.89		6.3	4.5	12.5	9.78
110	67.17	19.82	0.61	0.30	2.40	0.03	0.20	1.22	5.90	0.47	1.71	0.81	0.47	40.2	27.2	12.8	10.6	0.43	6.4	0.9	27.1	5.1	4.6	8.1	9.79
130	65.25	21.10	0.58	0.39	1.84	0.02	0.22	1.87	5.81	0.49	1.26	0.50	0.40	42.5	22.1	10.7	16.4	0.54	5.1	0.87		5.7	4.7	6.9	9.23
150	65.68	21.82	0.59	0.32	1.86	0.02	0.20	2.04	5.63	0.42	1.52	0.47	0.31	46.5	21.9	7.2	17.8	0.42	4.3	0.7		5.3	4.7	5.1	8.68
170	69.31	20.18	0.60	0.31	1.50	0.03	0.17	1.81	5.77	0.35	1.64	0.54	0.33	39.4	26.9	12.6	15.9	0.41	6.4	0.54		3.8	4.7	4.2	9.76
190	67.17	19.22	0.70	0.28	1.79	0.01	0.27	1.35	5.81	0.32	2.10	0.95	0.40	34.2	25.9	15.5	11.6	0.39	10.2	0.46		6.2	4.6	5.3	15.19
210	68.03	19.31	0.64	0.31	1.42	0.01	0.24	1.37	6.23	0.33	1.73	0.75	0.44	34	25.9	17.9	11.8	0.44	8.5	0.41	47.8	5.6	4.6	5.2	13.94

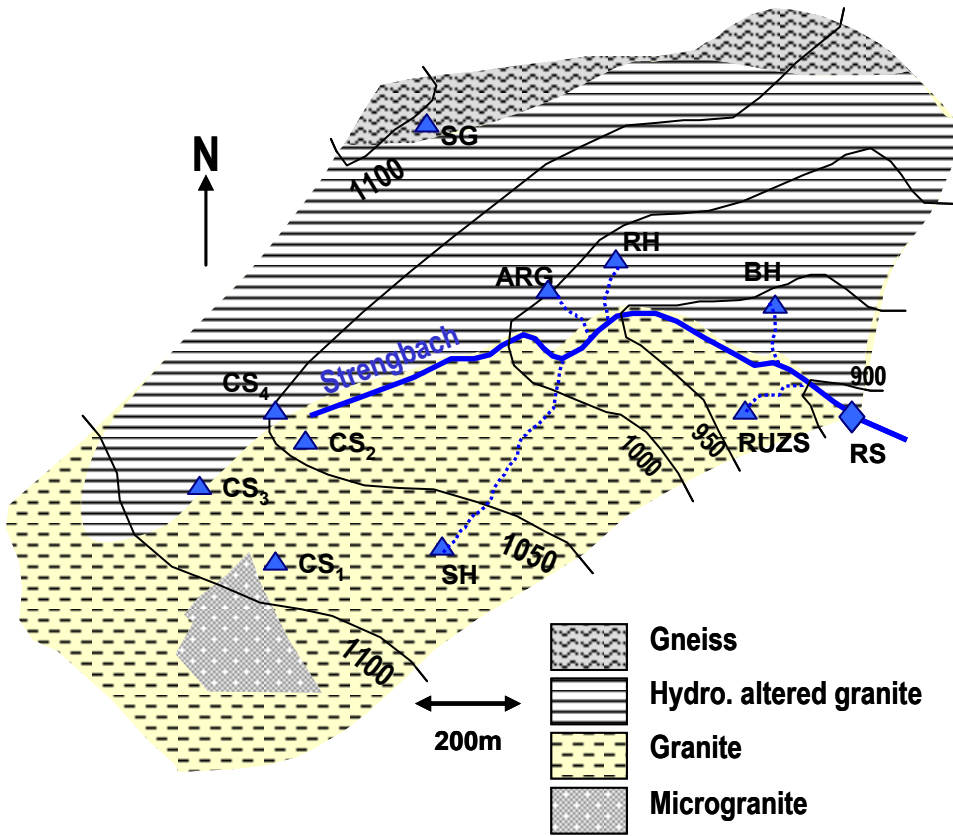
Soils under beeches - Southern slope (1)																									
depth	SiO2	Al2O3	MgO	CaO	Fe2O3	MnO	TiO2	Na2O	K2O	P2O5	Mg/Ca	Mg/Na	Ca/Na	muscovite	Quartz	K-Feld	plagio	apatite	Smectite	amorph	smectite (%)	OM	pH	Clays	CEC
cm	%	%	%	%	%	%	%	%	%	%	%	%	%	%	%	%	%	%	%	%	in clay fract.	%		%<2µm	cmol/kg
4	74.45	14.21	0.33	0.18	1.21	0.01	0.33	1.90	4.77	0.25	1.54	0.28	0.18	18.9	39.5	18.9	14.7	0.15	4.4	0.54	14.7	12	4.0	13.3	7.86
15	72.52	15.87	0.34	0.13	1.27	0.01	0.31	1.85	5.41	0.22	2.23	0.30	0.13	23.9	36.5	20	13.6	0.1	3.8	0.41		6.7	4.1	11.6	7.7
35	69.10	15.98	0.35	0.10	2.16	0.04	0.29	1.70	4.96	0.60	2.99	0.34	0.11	23.1	35.1	17.8	12.5	0.05	4.3	2.14		12.3	4.6	10.7	8.00
52.5	66.96	17.53	0.40	0.13	2.52	0.05	0.31	1.81	4.98	0.45	2.65	0.36	0.14	26.3	31.7	15.9	13.4	0.1	5	2.7	22.2	11.9	4.8	8.7	5.02
77.5	65.03	18.61	0.47	0.16	2.85	0.06	0.30	1.91	4.96	0.57	2.46	0.40	0.16	28.7	28.6	14.4	14.3	0.15	6.1	2.89		10.9	4.8	6.3	4.24
100	66.10	18.82	0.55	0.22	2.39	0.08	0.36	1.67	5.24	0.40	2.14	0.53	0.25	31	29.5	14.7	11.8	0.27	7.6	1.63	27.7	7.7	4.8	4.2	4.08
122.5	65.25	19.48	0.56	0.26	1.96	0.08	0.29	1.83	5.34	0.42	1.83	0.50	0.27	33.4	27.3	13.9	13.1	0.33	7.4	1.22		7.5	4.8	3.1	3.6
150	63.54	20.46	0.55	0.32	2.72	0.11	0.28	2.22	5.52	0.45	1.45	0.40	0.28	33.8	22.7	14.8	16.6	0.4	7.1	1.43		6	4.9	2.5	2.6
177.5	64.82	19.35	0.48	0.26	2.85	0.10	0.24	2.47	5.48	0.41	1.56	0.32	0.20	28.1	23.3	17.9	19.1	0.28	6.5	1.17		5.2	4.9	1.8	2.12
177.5	65.89	18.31	0.45	0.29	2.83	0.10	0.28	2.44	5.36	0.44	1.30	0.30	0.23	24	25.3	19.5	19	0.33	6.5	1.19		5.1	4.9	1.6	1.79
200	62.25	20.22	0.55	0.33	3.73	0.15	0.33	2.59	5.04	0.52	1.39	0.34	0.25	31.9	20.9	12.7	20.2	0.39	7.4	1.48	19.8	6.2	4.9	2.1	1.79

Soils - Gneiss (2)																									
depth	SiO2	Al2O3	MgO	CaO	Fe2O3	MnO	TiO2	Na2O	K2O	P2O5	Mg/Ca	Mg/Na	Ca/Na	muscovite	Quartz	K-Feld	plagio	apatite							
cm	%	%	%	%	%	%	%	%	%	%	%	%	%	%	%	%	%	%	%	%		%			
30	62.84	15.25	1.00	0.20	5.72	0.15	0.77	0.42	3.44	0.43	4.22	3.87	0.92	nd	nd	nd	nd	nd	nd						
65	69.61	15.20	1.35	0.13	5.27	0.09	0.71	0.38	3.93	0.24	8.77	5.77	0.66	nd	nd	nd	nd	nd	nd						
135	68.00	15.41	1.22	0.09	5.99	0.09	0.70	0.25	4.23	0.23	11.44	7.93	0.69	nd	nd	nd	nd	nd	nd						
175	71.88	15.61	1.02	0.24	3.11	0.04	0.56	0.05	4.71	0.23	3.59	33.16	9.24	nd	nd	nd	nd	nd	nd						
225	64.97	16.11	0.86	0.12	9.26	0.16	0.59	0.10	4.69	0.19	6.05	13.98	2.31	nd	nd	nd	nd	nd	nd						

Bedrock - average value (1), (2), this study																									
cm	SiO2	Al2O3	MgO	CaO	Fe2O3	MnO	TiO2	Na2O	K2O	P2O5	Mg/Ca	Mg/Na	Ca/Na	muscovite	Quartz	K-Feld	plagio	apatite							
	%	%	%	%	%	%	%	%	%	%	%	%	%	%	%	%	%	%	%	%		%			
Northern slope	75.38	14.50	0.45	0.29	1.38	0.03	0.19	0.98	6.19	0.31	1.31	0.75	0.57	29	49	19	2	0.5							
Southern slope	74.13	14.32	0.26	0.36	0.98	0.01	0.18	2.87	5.70	0.33	0.61	0.15	0.24	13	34	30	22	0.5							
Gneiss	65.08	17.95	2.55	0.20	7.59	0.07	0.89	0.55	4.13	0.12	10.63	7.54	0.71	nd	nd	nd	nd	nd	nd						

921
922
923
924
925
926

Table 4: Chemical and mineralogical compositions of soils and bedrocks from the Strengbach watershed. (1): Fichter, 1997, (2): El Gh’Mari, 1995.



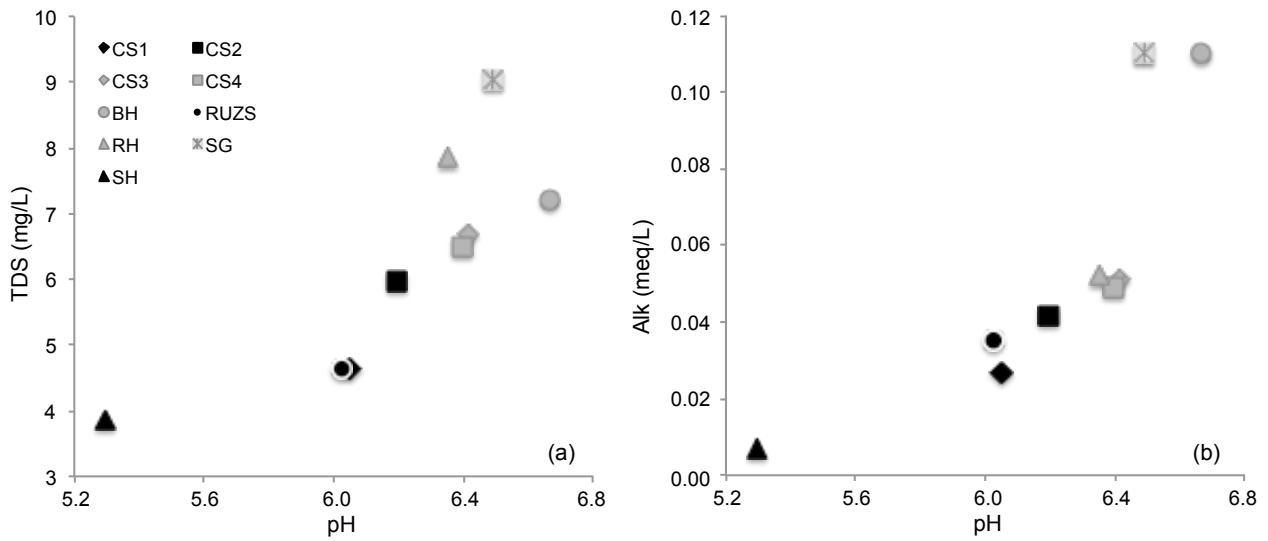
928

929 Fig. 1: Map of the Strengbach catchment showing the principal lithological units and the location of
 930 the 10 studied springs (SG, RH, ARG, BH, CS₁, CS₂, CS₃, CS₄, SH, RUZS). RS corresponds to
 931 the Strengbach stream at the outlet of the studied catchment.

932

933

934



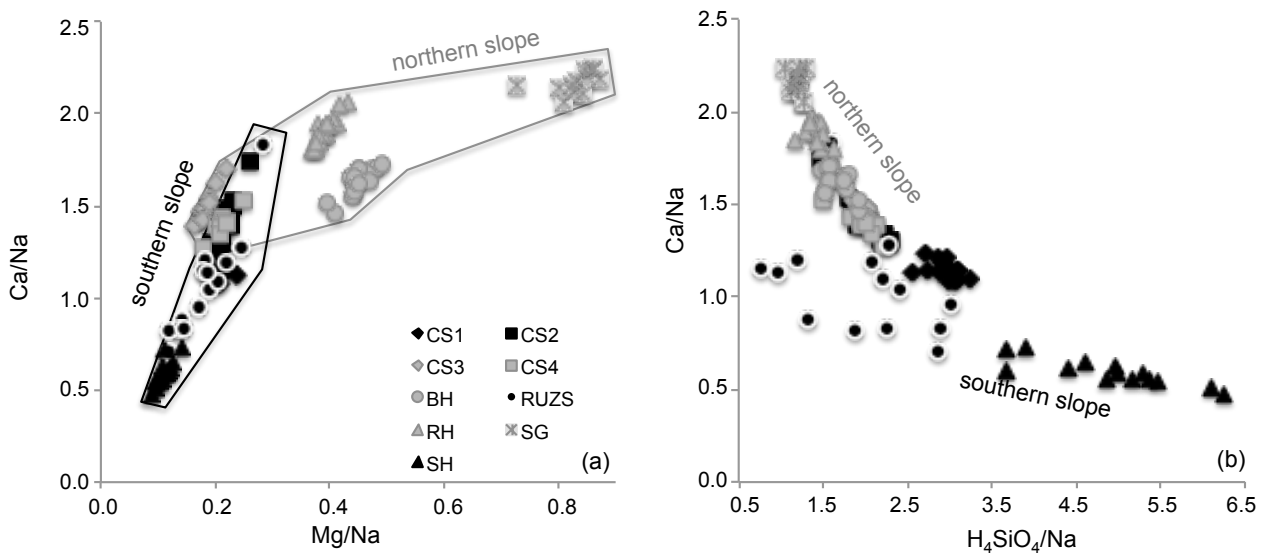
935

936 Fig. 2: Physico-chemical characteristics of the different source waters of the Strengbach watershed

937 (average values for the period 2004-2006). a) pH vs TDSw and b) pH vs Alk.

938

939



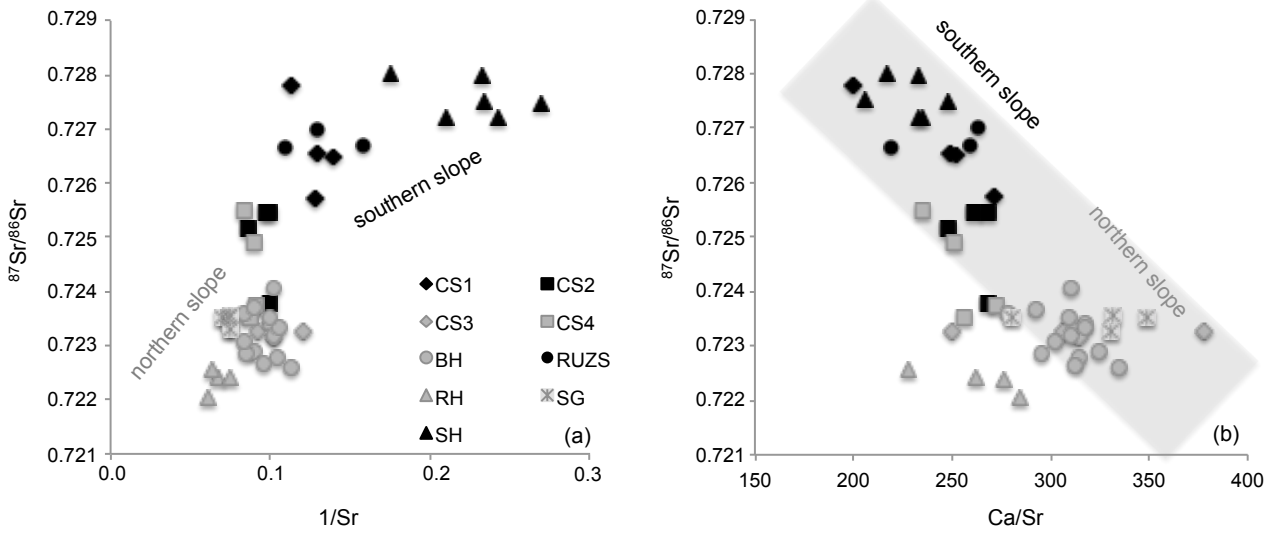
940

941 Fig. 3: Major element concentration ratios of the 9 different individual source waters of the

942 Strengbach watershed. a) Ca/Na vs Mg/Na and b) Ca/Na vs Si(OH)₄/Ca. In each diagram the spring

943 waters from the southern slope show different compositions than those from the northern slope.

944

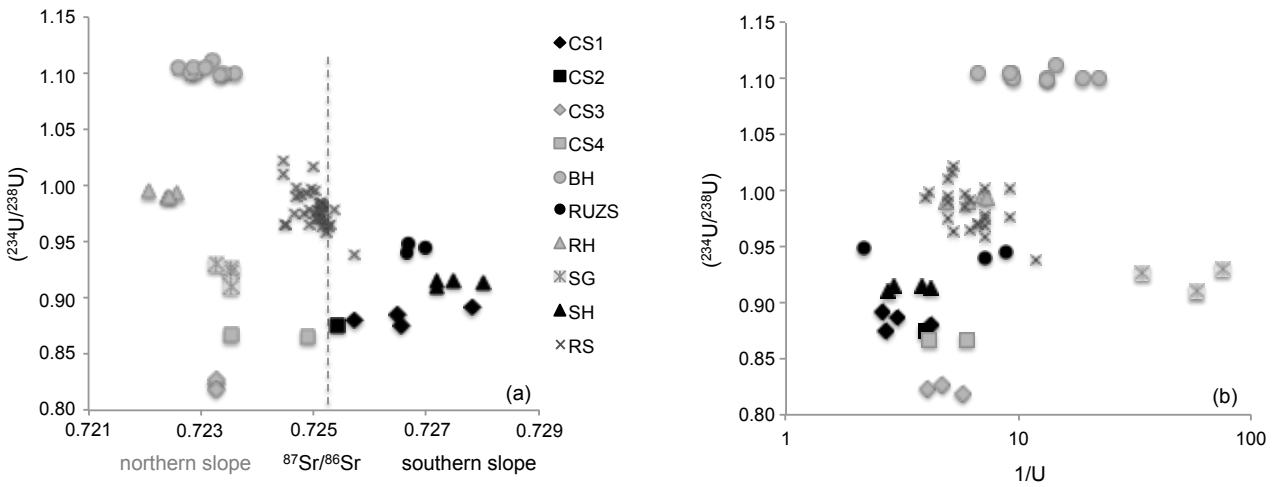


945

946 Fig. 4: Relationships between $^{87}\text{Sr}/^{86}\text{Sr}$ isotope ratios and a) $1/\text{Sr}$ (ppb); b) Ca/Sr (ppb/ppb). The
 947 isotope ratios allow a clear distinction between northern and southern slope sources.

948

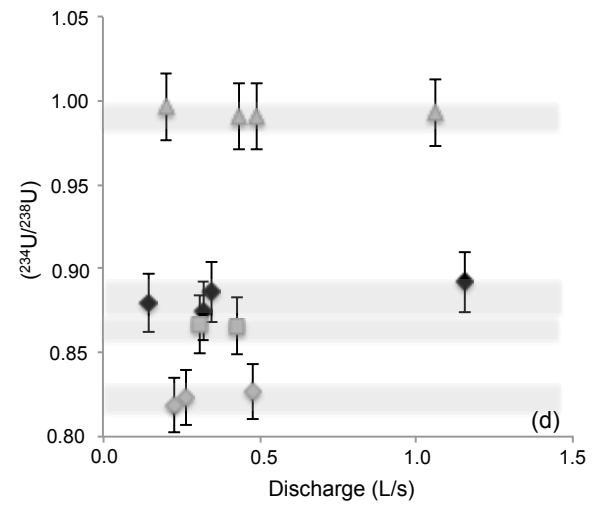
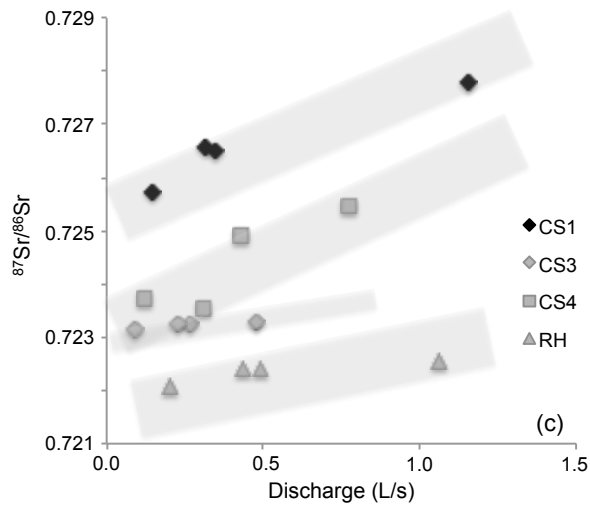
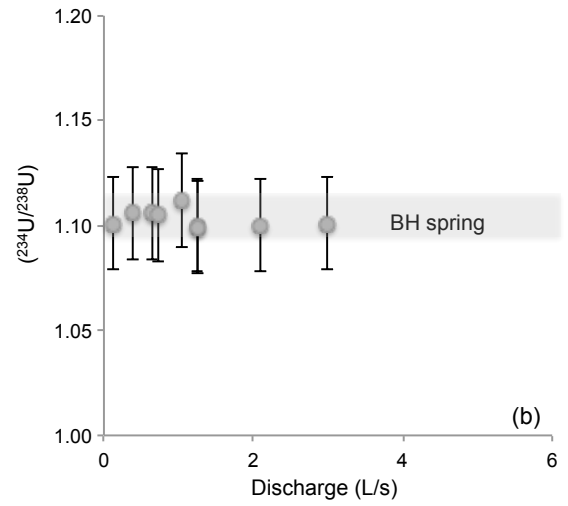
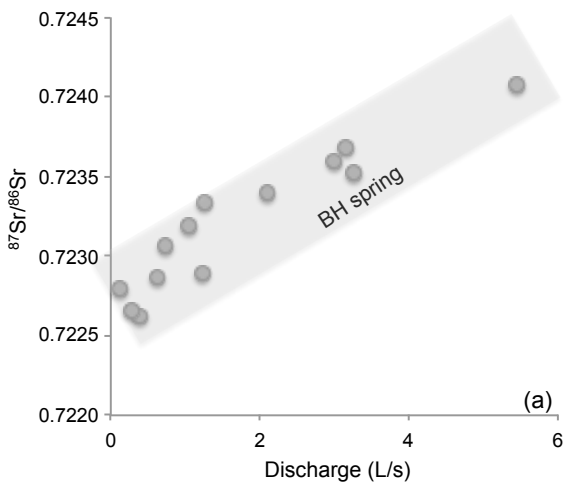
949



950

951 Fig. 5: Relationship between $(^{234}\text{U}/^{238}\text{U})$ AR and a) $1/\text{U}$ and, b) $^{87}\text{Sr}/^{86}\text{Sr}$. In contrast to Sr isotopic
 952 compositions, the U AR of springs do not allow to distinguish between the northern and southern
 953 slopes.

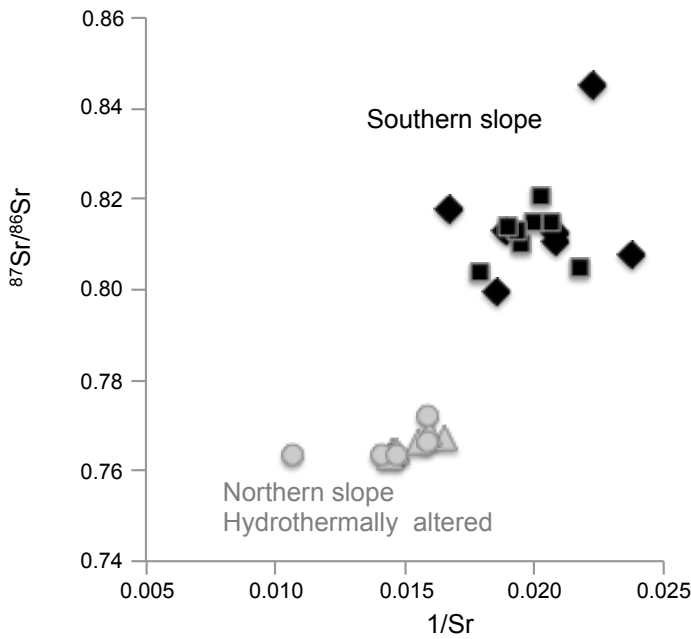
954



955

956 Fig. 6: $^{87}\text{Sr}/^{86}\text{Sr}$ and $(^{234}\text{U}/^{238}\text{U})$ AR vs discharge for the springs BH, CS1, CS3, CS4 and RH from
 957 the Strengbach watershed.

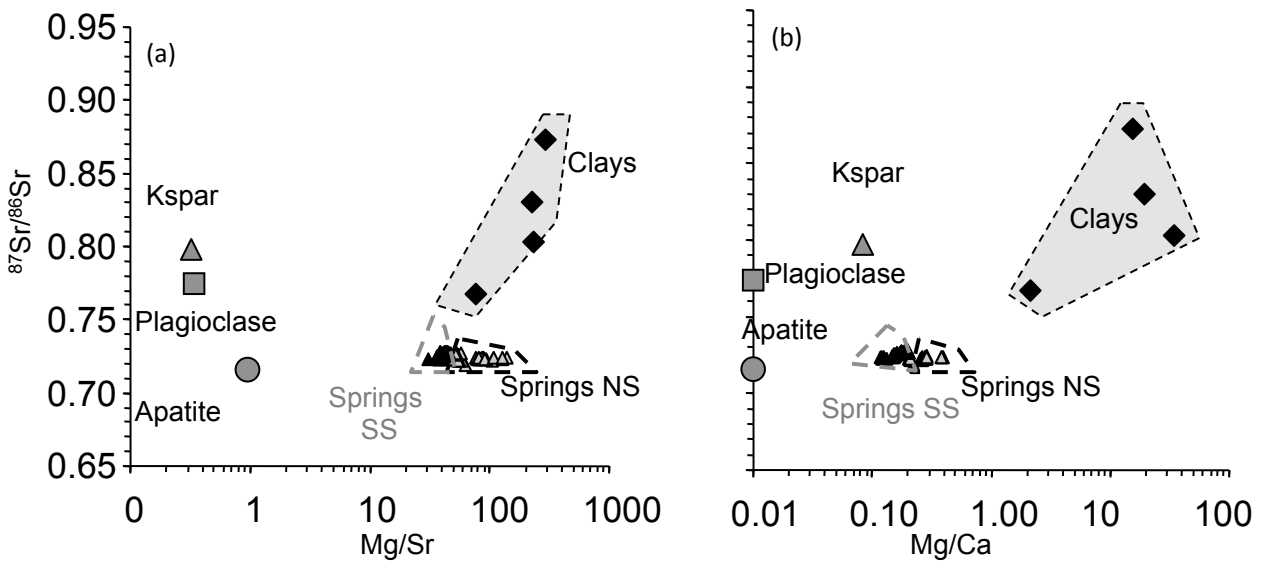
958



960

961 Fig. 7: $^{87}\text{Sr}/^{86}\text{Sr}$ vs $1/\text{Sr}$ for the soil and saprolite samples from the Strengbach watershed. The
 962 samples from the northern slope and those from the southern slope are clearly different (Aubert,
 963 2001; Stille et al., 2009 ; Prunier, 2008).

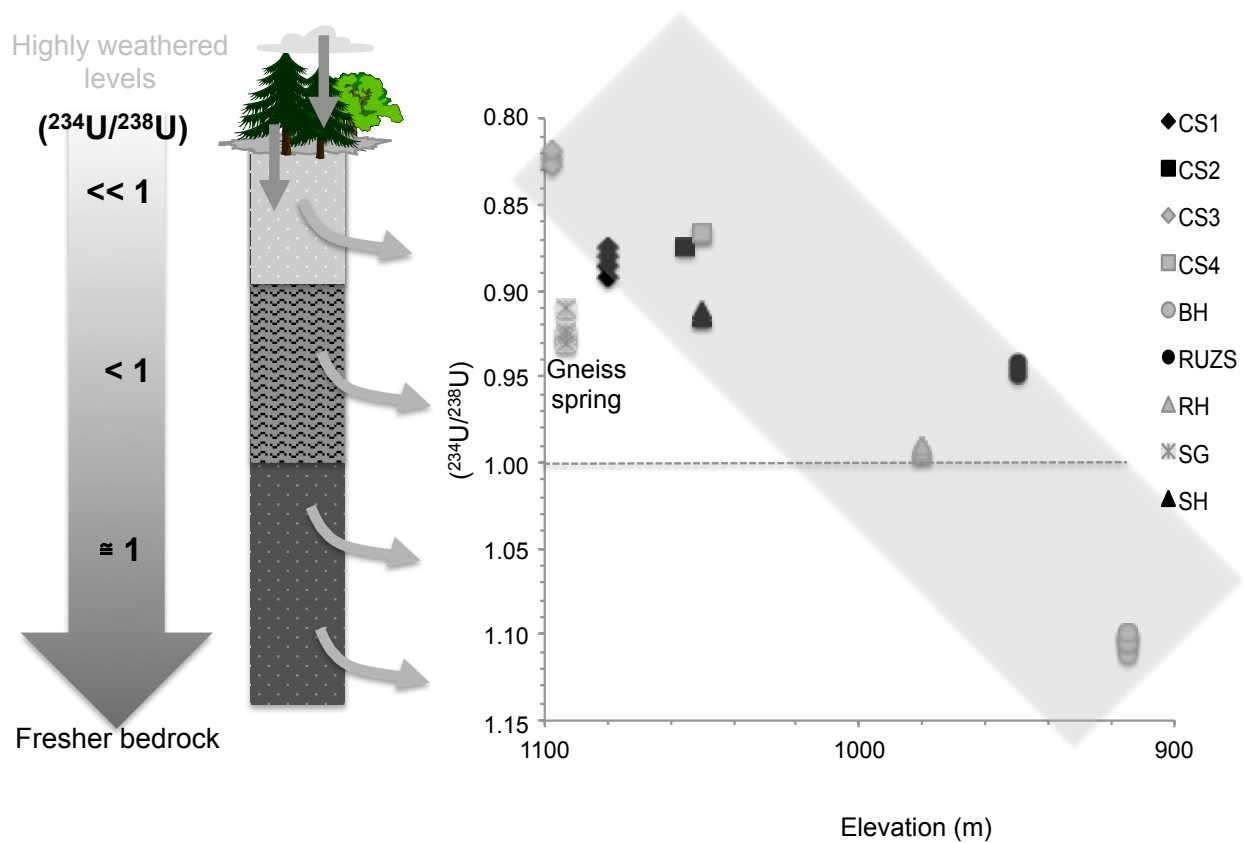
964



965

966 Fig. 8: $^{87}\text{Sr}/^{86}\text{Sr}$ vs Mg/Ca (a) and Mg/Si (b) for the spring waters (NS = northern slope and
 967 SS=southern slope), primary minerals of the granite (Aubert et al.. 2001) and clays from soils
 968 (Prunier, 2008).

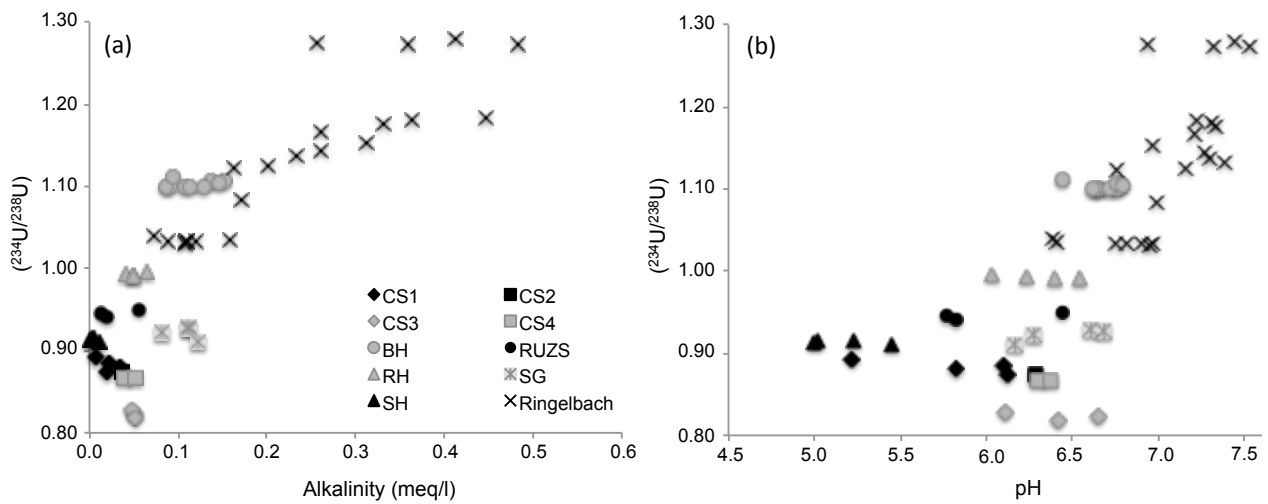
969



970

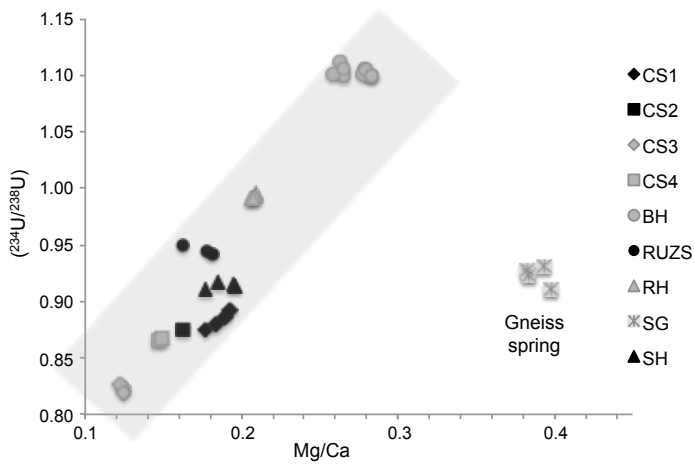
971 Fig. 9: $(^{234}\text{U}/^{238}\text{U})$ AR of springs vs elevation. The U AR increase with decreasing altitude at the
 972 catchment scale.

973



974

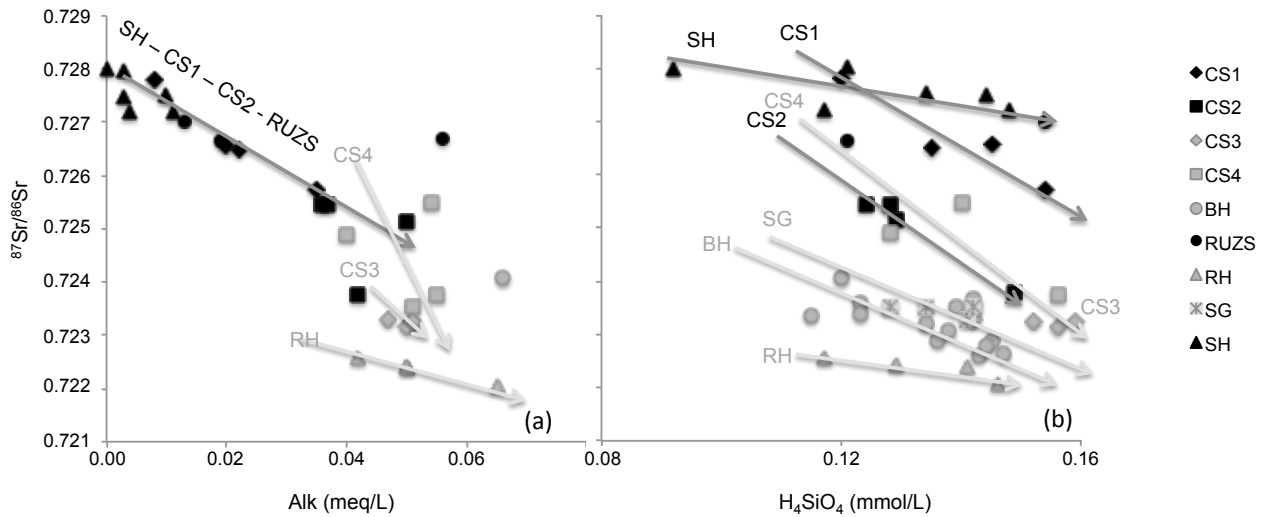
975 Fig.10: Variations of $(^{234}\text{U}/^{238}\text{U})$ AR vs a) alkalinity and b) pH in the springs from the Strengbach
 976 and Ringelbach (Shaffauser et al., 2014) watersheds.



977

978 Fig. 11: Variations of ($^{234}\text{U}/^{238}\text{U}$) AR vs Mg/Ca ratio in the springs. The U AR are positively
 979 correlated with the Mg/Ca ratios.

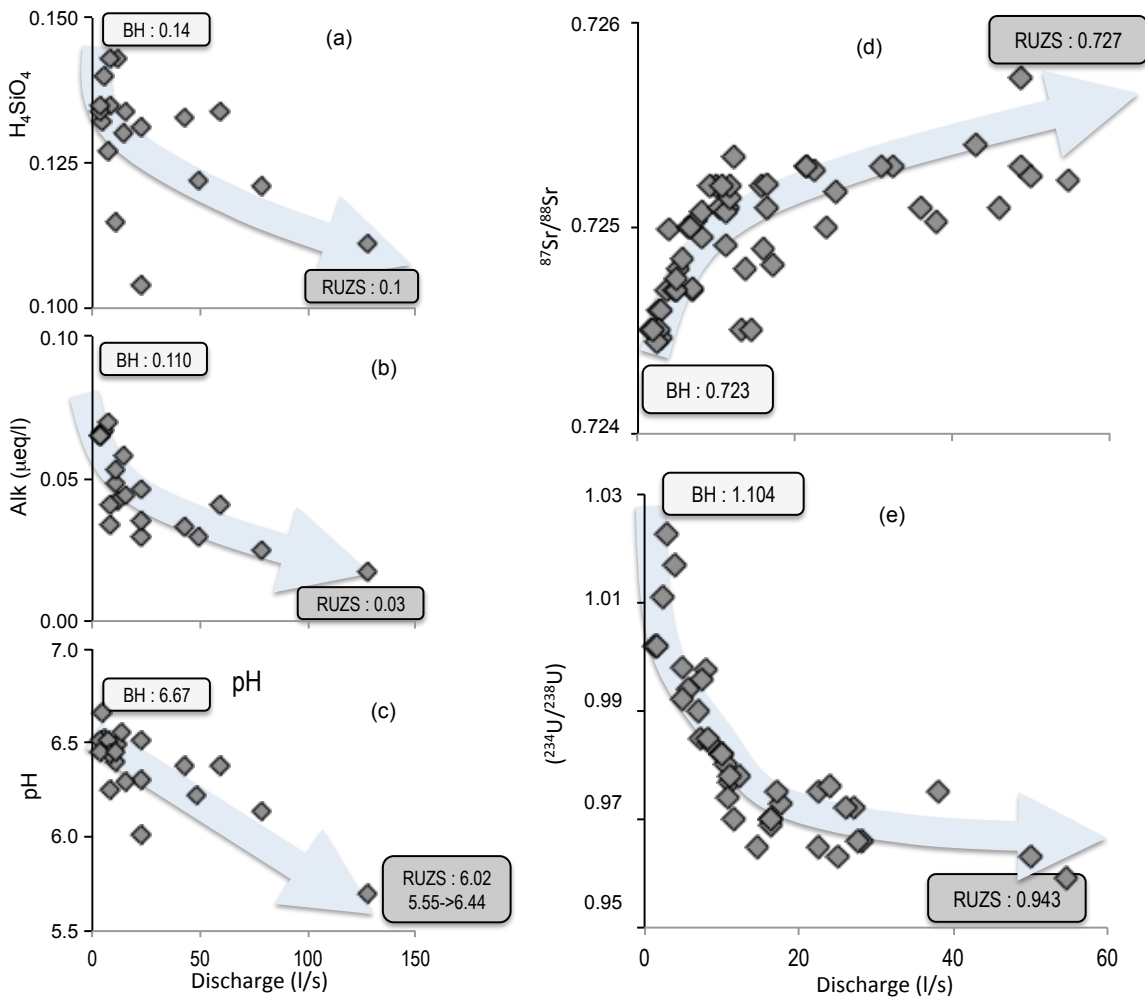
980



981

982 Fig. 12: $^{87}\text{Sr}/^{86}\text{Sr}$ vs alkalinity (a) and Si concentrations (b) for the springs from the Strengbach
 983 watershed. For each of the individual spring the $^{87}\text{Sr}/^{86}\text{Sr}$ ratios decrease with increasing alkalinity
 984 and Si content.

985



986

987 Fig. 13: H_4SiO_4 concentration (a), alkalinity (b), pH (c), $(^{234}U/^{238}U)$ AR (d) and $^{87}Sr/^{86}Sr$ (e) vs
 988 discharge at the outlet for the 2004-2006 period (additional data from Riotte et al. (1999) and
 989 Aubert et al., (2002)).

990

991

992

993